

**Ischemia – Reperfusion Destabilizes Rhythmicity in Immature  
Atrio-Ventricular Pacemakers: A Predisposing Factor for  
Postoperative Arrhythmias**

**by**

**YuQi Cici Chenliu**

B.Sc., Simon Fraser University, 2013

Thesis Submitted in Partial Fulfillment of the  
Requirements for the Degree of  
Master of Science

in the

Department of Biomedical Physiology and Kinesiology  
Faculty of Science

**© YuQi Cici Chenliu 2016**

**SIMON FRASER UNIVERSITY**

**Spring 2016**

All rights reserved.

However, in accordance with the *Copyright Act of Canada*, this work may be reproduced, without authorization, under the conditions for Fair Dealing. Therefore, limited reproduction of this work for the purposes of private study, research, education, satire, parody, criticism, review and news reporting is likely to be in accordance with the law, particularly if cited appropriately.

# Approval

**Name:** YuQi Cici Chenliu  
**Degree:** Master of Science  
**Title:** *Ischemia – Reperfusion Destabilizes Rhythmicity in Immature Atrio-Ventricular Pacemakers: A Predisposing Factor for Postoperative Arrhythmias*

**Examining Committee:** **Chair:** Dr. Will Cupples  
Professor

**Dr. Glen F Tibbits**  
Senior Supervisor  
Professor

---

**Dr. Shubhayan Sanatani**  
Supervisor  
Head  
Division of Cardiology  
BC Children’s Hospital

---

**Dr. Thomas Claydon**  
Supervisor  
Associate Professor

---

**Dr. Charles Krieger**  
External Examiner  
Professor

---

Date Defended/Approved:

April 26, 2016

---

## Ethics Statement



The author, whose name appears on the title page of this work, has obtained, for the research described in this work, either:

- a. human research ethics approval from the Simon Fraser University Office of Research Ethics

or

- b. advance approval of the animal care protocol from the University Animal Care Committee of Simon Fraser University

or has conducted the research

- c. as a co-investigator, collaborator, or research assistant in a research project approved in advance.

A copy of the approval letter has been filed with the Theses Office of the University Library at the time of submission of this thesis or project.

The original application for approval and letter of approval are filed with the relevant offices. Inquiries may be directed to those authorities.

Simon Fraser University Library  
Burnaby, British Columbia, Canada

Update Spring 2016

## **Abstract**

Post-operative arrhythmias, such as Junctional Ectopic Tachycardia (JET) and atrioventricular (AV) block, are serious post-operative complications for children with congenital heart disease <sup>1</sup>. We hypothesize that these arrhythmias arise within the AV node because of an ischemia-reperfusion (I/R) insult in the setting of immature myocytes, exacerbated by post-operative inotropy.

Rabbit whole heart models of post-operative arrhythmias were generated, focusing on three primary risk factors: age, I/R exposure and the application of dopamine, an inotropic agent. Using optical mapping technology, neonatal rabbit hearts were found to experience persistent post-ischemia arrhythmias of differing severity while mature hearts exhibited no arrhythmias or transient ones, when the three risk factors were varied.

Compared to rabbit mature hearts, rabbit neonatal whole hearts demonstrated a susceptibility to I/R insults resulting in alterations in automaticity. An analogous susceptibility may predispose human neonates to post-operative arrhythmias such as JET and AV block.

**Keywords:** Automaticity; atrio-ventricular node; neonate heart; Junctional Ectopic Tachycardia; AV block; ischemia reperfusion

*This thesis is dedicated to my parents, who have always  
believed in me, who gave me the freedom to learn and  
grow.*

## **Acknowledgements**

There are several individuals I'd like to acknowledge and extend my gratitude to. First and foremost, I'd like to thank Dr. Tibbits. His guidance, support and patience have been crucial to the success of not only my graduate studies but also my growth as an individual. Dr. Tibbits is always willing to entertain questions, provide appropriate guidance and push me to think critically. I am very lucky to have him as my senior supervisor and am grateful for the privilege of studying under him.

I would also like to extend my gratitude towards my committee members Dr. Sanatani and Dr. Claydon. Dr. Sanatani was a valuable mentor who guided my research and helped to frame its clinical relevance and impact. He always found time in his busy schedule to entertain my questions about the heart and otherwise. I am thankful for Dr. Claydon in providing key insights for my proposal and making important suggestions that directed me to think about my research more critically.

I'd also like to thank my lab supervisor Helen who supported me both emotionally and professionally throughout the past three years. She, being a strong woman, has encouraged and motivated me to live freely, work hard and to move forward without fear or hesitation, and in her own words, "just do it".

Finally, I'd like to acknowledge my lab members including Lilian Lee, Grace Chun, Jeff Chen, and Mike Xu who have all impacted my graduate life. They have celebrated and despaired with me, and were an integral part of my graduate experience. Additionally, I'd like to thank Eric Lin for setting up the optical mapping equipment and the analytical software which was fundamental to the operation of this study.

# Table of Contents

Approval.....	ii
Ethics Statement.....	iii
Abstract.....	iv
Dedication.....	v
Acknowledgements.....	vi
Table of Contents.....	vii
List of Tables.....	ix
List of Figures.....	ix
List of Acronyms.....	x
<b>Chapter 1. Introduction .....</b>	<b>1</b>
1.1. Background.....	1
1.2. Post-operative arrhythmias.....	2
1.3. Cardiopulmonary Bypass and Ischemia Reperfusion Insult .....	3
1.4. Cardiac Electrophysiology .....	5
1.4.1. Overview of cardiac anatomy and electrophysiology .....	5
1.4.2. Theories of nodal automaticity .....	7
1.4.3. Protein expression and nodal differences in automaticity.....	9
<b>Chapter 2. Thesis Objectives .....</b>	<b>11</b>
<b>Chapter 3. Experimental Design and Methods .....</b>	<b>12</b>
3.1. Langendorff Technique.....	12
3.2. Optical Mapping of the Heart .....	13
3.3. Methods .....	14
3.3.1. Animals .....	14
3.3.2. Heart Excision .....	14
3.3.3. Whole Heart Optical Mapping Study .....	15
3.3.4. Solutions.....	15
3.3.5. Exclusion Criteria.....	16
3.3.6. Definitions of Arrhythmia.....	16
3.4. Experimental Protocols.....	17
3.4.1. Study 1: Effect of experimental procedures on cardiac performance .....	17
3.4.2. Study 2: Effect of age on reperfusion arrhythmias .....	17
3.4.3. Study 3: Effect of post ischemia DA administration.....	18
3.4.4. Study 4: Effect of ischemic duration on reperfusion arrhythmias.....	18
3.5. Analysis.....	18
<b>Chapter 4. Results .....</b>	<b>19</b>
4.1. I/R induced arrhythmias were dependent on maturation stage .....	19
4.1.1. 10-d (neonate) - reperfusion time (5 min).....	19
4.1.2. 10-d (neonate) - reperfusion time (10 min).....	20

4.1.3.	56-d (mature) – reperfusion time (5, 10 min).....	20
4.2.	Post ischemic administration of DA did not influence I/R induced arrhythmias.....	21
4.3.	Increased I/R duration exacerbate arrhythmias to a greater degree in neonate hearts than in mature hearts .....	21
4.3.1.	90 min GI, 10-d (neonate).....	21
4.3.2.	90 min GI, 56-d (mature) .....	22
4.4.	Summary of results.....	22
 <b>Chapter 5. Discussion .....</b>		<b>23</b>
5.1.	Methodology.....	23
5.1.1.	Animal Models.....	23
5.1.2.	Langendorff retrograde perfusion technique .....	24
5.1.3.	Optical Mapping of the rabbit heart.....	24
5.2.	Reperfusion Arrhythmias .....	25
5.2.1.	Ionic Basis of Ischemia Reperfusion.....	27
5.3.	Future Directions .....	28
5.3.1.	Dual Optical Mapping .....	28
5.3.2.	Endocardial Mapping.....	30
 <b>Chapter 6. Conclusion.....</b>		<b>31</b>
 <b>References .....</b>		<b>48</b>



## List of Tables

Table 1:	Study 1 control experiments (hearts perfused for 2 hours continuously, (+) 20 $\mu$ M DA).....	32
Table 2:	Study 2 (30 min GI, reperfusion, (+) 20 $\mu$ M DA) .....	33
Table 3:	Study 3 (30 min GI, reperfusion, (-) DA) .....	34
Table 4:	Study 4 (90 min GI, reperfusion, (+) 20 $\mu$ M DA) .....	35
Table 5:	10-d control experiment (no IM, 30 min GI, reperfusion with KHB) .....	36

## List of Figures

Figure 1:	Cardiopulmonary bypass schematic.....	37
Figure 2:	Cardiac conduction axis .....	38
Figure 3:	Location of AVN pacemakers within the AVJ.....	39
Figure 4:	Optical mapping set up showing the optical pathways.....	40
Figure 5:	Definition of arrhythmias and representative optical action potential traces.....	41
Figure 6:	Representative regions of interest (ROI) analysis and control (Con) optical action potentials (OAP). .....	42
Figure 7:	Study protocols .....	43
Figure 8:	Average heart rate response, in whole heart optical mapping, to control (10-d & 56-d) .....	44
Figure 9:	Proportional representation of rhythmic responses, comparing age and ischemic duration .....	45
Figure 10:	Proportional representation of rhythmic responses, comparing age and post ischemia inotropy.....	46
Figure 11:	Optical mapping chamber .....	47

## List of Acronyms

AV	Atrioventricular
AVB	Atrioventricular Block
AVJ	Atrioventricular Junction
AVN	Atrioventricular Node
CaMKII	Calmodulin-dependent Protein Kinase II
CCS	Cardiac Conduction System
CHD	Congenital Heart Disease
DA	Dopamine
DD	Diastolic Depolarization
ECF	Extracellular Fluid
GI	Global Ischemia
GUCH	Grown Up Congenital Heart Disease
HCN	Hyperpolarization Activated Cyclic Nucleotide Gated Channel
I/R	Ischemia Reperfusion
IM	Ischemia Mimetic
JET	Junctional Ectopic Tachycardia
KHB	Krebs Henseleit Buffer
NCX	Sodium Calcium Exchanger
OM	Optical Mapping
OPA	Optical Action Potential
ROI	Region of Interest

SAN	Sinoatrial Node
SERCA	Sarcoplasmic Reticulum ATPase
SOICR	Ca <sup>2+</sup> -Overload Induced SR Release of Ca <sup>2+</sup>
SR	Sarcoplasmic Reticulum
SVT	Supraventricular Tachycardia
TVAD	Tachycardia with VA Dissociation

# Chapter 1.

## Introduction

### 1.1. Background

Congenital Heart Diseases (CHD) include severe heart defects that are present at birth, occurring on average in 8 out of 1000 live births<sup>2</sup> or approximately 1.35 million births per year worldwide. Congenitally malformed hearts can result from both genetic and non-genetic factors<sup>3</sup>. At present, significant public health efforts in education and prevention has been focused primarily on the more predictable and easily preventable non-genetic causes rather than the more difficult genetic factors. Factors such as environmental toxins, teratogens and substance abuse have been identified as major causes of CHD<sup>2,4</sup>. Additionally, maternal obesity and chronic health issues such as diabetes and hypercholesterolemia have also been recognized as risk factors for CHD<sup>3</sup>. Despite vigorous prevention efforts, the incidence of CHD is increasing in the global population<sup>2,5</sup>.

Advances in medical technology and surgical innovations have significantly improved the survival rate and treatment outcome of CHD patients who are usually very young when the medical intervention is initially undertaken<sup>2</sup>. However, these treatments are costly both financially and in terms of health and wellbeing. The pediatric CHD patients who are successfully treated often require long term expert care, continuous drug therapies and ongoing medical monitoring as a result of disease and intervention related complications. One of the most severe post-cardiac corrective surgery complications is post-operative arrhythmias<sup>6</sup>. The occurrence of these arrhythmias significantly compromise the patient's medical outcome, both short-term and long-term<sup>7</sup>. Follow up studies have revealed that patients who developed post-operative arrhythmias also have worse long-term medical outcomes than patients who did not develop post-

operative arrhythmias<sup>2,7</sup>. These successfully treated, now “grown up congenital heart disease” (GUCH) patients<sup>2</sup> face a future of uncertain health and well-being. As their numbers grow, it has become crucial to understand the underlying causes of these types of post-operative arrhythmias in order to improve the quality of life for surviving patients and the socioeconomic well-being of the medical system as a whole.

## **1.2. Post-Operative Arrhythmias**

Post-operative arrhythmia is a serious complication that can occur following surgical correction of congenital heart defects in infants. These arrhythmias are generally poorly tolerated by pediatric patients due to their young age and the severity of their disease and the post-operation period is a particularly sensitive time in terms of infant morbidity and recovery. Various studies have indicated that post-operative arrhythmias occur in 8% – 48% in the patient population<sup>8-12</sup>. To date, surgical substrates have been the primary suspect in causing post-operative arrhythmias, with higher frequencies of arrhythmias being associated with increased surgical complexity and specific surgical techniques<sup>8,11-13</sup>. Additionally, certain types of defects requiring similar surgical procedures, such as ventricular septal defects, have been correlated with the onset of specific types of post-operative arrhythmias such as Junctional Ectopic Tachycardia (JET). However, the correlation between the various categories of arrhythmias and the types of surgical interventions is still not clearly understood<sup>8,12-15</sup>. This lack of understanding of the relationship between post-operative arrhythmias and surgical intervention, coupled with the arrhythmias’ multivariate nature and heterogeneous phenotypes, means the etiology of post-operative arrhythmias is fundamentally unknown.

Post-operative arrhythmias can manifest in many ways. The main types of post-operative arrhythmias are JET, supraventricular tachycardia (SVT), and conduction blocks (such as atrioventricular block [AVB]). JET is a malignant arrhythmia which is characterized by a normal QRS complex with ventricular contraction rates greater than the upper limits of sinus rhythm and normally accompanied by ventriculoatrial (VA) dissociation<sup>16-18</sup>. While JET is technically categorized as an SVT, it is usually treated independently because of its severity and unique pathological phenotype. Other forms of

SVT include re-entrant tachycardia with 1:1 AV conduction or retrograde p waves which can be recorded on electrocardiograms. Premature ventricular complexes, which are extra systoles initiated by an abnormal focus within the ventricular conduction axis, are documented as post-operative arrhythmia if they exceed 10 abnormal beats per minute (bpm) in most studies. Other potential post-operative arrhythmias include atrial flutter, atrial tachycardia, sick sinus syndrome and AVB<sup>8-12,15,19</sup>. Post-operative arrhythmias are exacerbated by positive inotropic agents which is why many centers try to avoid exogenous inotropic treatments, such as the use of cardiac glycosides,  $\beta$ -adrenoreceptor agonists, and calcium sensitizers, in the post-operative course. Incidence of post-operative arrhythmias differ from study to study; however, post-operative SVT, JET, and AVB are more frequently observed<sup>8-10,12,20</sup>.

To treat, a protocol to minimize exposure to exogenous catecholamines, limit hyperthermia, control pain and keep the patients sedated while the arrhythmias subside, is generally instituted. Pharmacological interventions are also employed if the arrhythmias persist and studies have shown some success with amiodarone<sup>10,11,15</sup>. Infants with conduction blocks are usually artificially paced and monitored and, if complete conduction blocks persist, permanent pacemakers are implanted. JET is one of the more difficult arrhythmias to treat because of the associated severe hemodynamic instability, leading to increased morbidity and mortality rates. Post-operative infants do not tolerate such rhythmic and hemodynamic disturbances well; therefore, effective management of JET is crucial for post-operative patients in the pediatric intensive care unit. However, while diagnoses have been well established and medical treatment options are increasingly effective, the underlying cause of post-operative arrhythmia is not understood.

### **1.3. Cardiopulmonary Bypass And Ischemia Reperfusion Insult**

Cardiopulmonary bypass (CPB) (Figure 1) is a procedure that diverts blood away from the heart, enabling effective surgical procedures to be performed on the heart by allowing blood to circulate and re-oxygenate outside of the heart and lungs during an operation. This allows the surgeon to work on the surface and within the chambers of the

quiescent, bloodless heart. In order to achieve this, the heart or the circulatory system must be cannulated on both the arterial and venous sides. Cannulations on the venous side aid in the drainage of blood from the heart and body into the pump reservoir<sup>21</sup> and cannulations on the arterial side aid in recirculating the blood and delivering nutrients to the rest of the body while bypassing the heart. Due to variations in surgical requirements and restraints, different cannulation techniques and locations are employed. Most commonly, the aorta or femoral artery are cannulated on the arterial side and the inferior vena cava and right atrium are cannulated on the venous side. The aorta is cross-clamped before the aortic cannula, and at a location above the coronary ostia, in a procedure known as aortic cross clamping (ACC) (Figure 1). Once the aorta is clamped, and coronary blood flow has ceased, the heart will experience ischemia; necessitating the employment of cardioprotective mechanisms. These mechanisms may include hypothermia (a cooling of the heart to reduce its metabolic needs), periodic reperfusion (restoration of blood flow), and/or infusion of cardioplegic solutions (normally high in  $K^+$  and  $Mg^{2+}$ ). Cardioplegia arrests the heart in a depolarized state to stop cardiac contraction and decrease metabolic demand and there are different cardioplegia solutions in use, conferring certain advantages or disadvantages depending on the components and their concentrations<sup>22</sup>. Infusion of a cardioplegic solution and induced hypothermia are often used in conjunction to delay the negative effects of ischemia, preserving cardiac function and tissue viability<sup>21</sup>. These steps are taken to prevent the known detrimental effects of ischemia/reperfusion (I/R) on the myocardium.

CPB has proven to be essential to open heart surgeries but the procedure is not without its drawbacks. It is well known that increased CPB duration is positively associated with increased morbidity; more specifically, in pediatric patients, increased CPB duration has been associated with poor recovery of cardiac function<sup>23</sup> and increased incidence in post-operative arrhythmias<sup>10,11,20</sup>. Elevated serum levels of cardiac-specific troponin I (TnI) and troponin C (TnC) are well established markers of myocardial damage with studies showing increased CPB duration is positively correlated to increased levels of TnI and TnC post-operatively<sup>24-26</sup>. In this lab, previous experiments on isolated single atrio-ventricular node (AVN) and sino-atrial node (SAN) cells have demonstrated the effects of I/R on spontaneous nodal activity<sup>27</sup>. Ischemia mimetic solutions selectively affect AVN cell automaticity (spontaneous activity) which may

explain the decreased cardiac conduction and increased AVB observed in infants after CPB surgery.

Besides damage to myocytes and contractile filaments within the myocytes, systemic inflammatory response is also linked to post-operative arrhythmias, particularly with accelerated rhythms<sup>28</sup>. In 2003, Seghaye<sup>28</sup> reviewed the clinical impact of systemic inflammation on infants and children undergoing cardiac malformation corrective surgeries and reported that patients who developed post-operative arrhythmias had significantly higher levels of pro-inflammatory cytokines such as interleukin-6 and interleukin-8. Histamine is an inflammation mediator that has pronounced effects on cardiac rhythmicity, causing accelerated sinus rhythm, induction of AVB and enhanced automaticity of ectopic pacemaker sites<sup>29</sup>. Seghaye's research confirmed that patients who developed various types of post-operative arrhythmias such as JET, AVB and accelerated junctional rhythms (AJR) had significantly elevated levels of histamine<sup>28,30</sup>. Furthermore, Zavec & Levi's study revealed that hearts can experience multiple types of arrhythmia in succession, as seen in post-operative infants who experience both conduction blocks and accelerated rhythms. Using genetically mutated mice, He et al<sup>31</sup> found that production of histamine is linked to ischemia induced sympathetic activity. This is in line with the theory that CPB induced increases in sympathetic activity would trigger an increase in histamine production as a neurotransmitter, and act directly on the pacemakers<sup>31</sup>. Together, evidence suggests that CPB related ischemia can trigger systemic inflammatory responses which are pro-arrhythmic.

## **1.4. Cardiac Electrophysiology**

### **1.4.1. Overview Of Cardiac Anatomy And Electrophysiology**

From a macroscopic perspective, in order to understand how cells interact and function as a unit, the fundamentals of the cardiac conduction system (CCS) must be first be discussed. The CCS has been studied for more than 100 years<sup>32</sup> and since then, a vast body of knowledge pertaining to the conduction system and cardiac automaticity has been amassed. Researchers are now able to identify specific molecular markers



within the conduction axis and describe their structures and functions as part of the CCS<sup>33</sup>.

In brief, electrical conduction through the CCS begins in the SAN and travels through the atria, activating atrial myocytes as it propagates. It is relayed to the ventricles by the AVN and from there, the electrical signal travels down the bundle of His and through the Purkinje fibers, towards the apex of the heart and activates the ventricular myocytes from apex to base<sup>32</sup> (Figure 2). In this manner, the electrical signals are regulated to ensure an “all or nothing” activation of the cardiomyocytes and resulting in a functional syncytium. The AV junction (AVJ) is the conducting region between the atria and ventricle, relaying cardiac electrical signals but also able to spontaneously depolarize. This region is extremely heterogeneous in terms of cellular morphology, protein expression, function and conducting properties<sup>34,35</sup>. While single cells have been isolated from the AVJ<sup>35</sup>, its membrane currents recorded<sup>35</sup>, and its electrical activities observed in mapping studies<sup>36</sup>, the underlying mechanisms of the AVJ’s function and electrophysiology are still not fully understood. Continued research into the functions and behaviour of the AVJ throughout the maturation process of the neonate, and particularly with respect to pathology and arrhythmias, is warranted.

Within the working myocardium, cellular activation is better understood. A wave of depolarization spreads from cell to cell via gap junctions and uniformly across the membrane surface. Once the activation threshold is reached, sodium channels ( $\text{Na}_v1.5$ ) are activated and rapidly depolarize the membrane. Then, following depolarization, the voltage sensitive L-type calcium channels ( $\text{Ca}_v1.2$ ) are activated, allowing calcium ions into the cell to induce further calcium release from the sarcoplasmic reticulum (SR). Next, the voltage sensitive, slow ( $\text{K}_v7.1$ ) and rapid ( $\text{K}_v11.1$  or HERG) potassium ion channels are activated to repolarize the membrane to its resting potential. Typically in human ventricular myocytes, an action potential lasts between 200 – 250 ms<sup>37</sup>.

Connected end-to-end, cardiomyocytes function as a working syncytium because of the way they are electrically and mechanically coupled by intercalated discs. Within the intercalated discs, gap junction proteins or connexins (Cx) are responsible for the cell-to-cell conduction of the electrical signal. Cx43 is found in the majority of gap

junctions in the working myocardium and is a low resistance, fast-conducting gap junction protein<sup>35,38</sup> while Cx45 is a gap junction protein with high resistance and low conductance, found mainly within the AV conduction axis. In species such as mouse, rat and rabbit, which are often used to model human cardiac conduction, another gap junction protein, Cx40 is expressed within the CCS as well<sup>39</sup>. Specifically, it is a part of the ventricular conduction pathways, primarily located at the distal end of the bundle of His and Purkinje fibers<sup>39</sup>. Connexin 40 seems to be important for AV conduction since Cx40 null animals present with conduction blocks<sup>39</sup>. Other gap proteins also exist within the myocardium; however, the aforementioned Cx40, 43 and 45 are broadly expressed across species and are known to play important functional roles within the CCS, with expression patterns indicating their involvement in the control and regulation of the rate and spread of electrical conduction. Specifically, signals tend to slow down through the AVJ but accelerate and can travel with less resistance elsewhere in the CCS.

A nodal-specific protein neurofilament-160 (NF-160) has been discovered in the rabbit<sup>34,35</sup> which, when combined with the use of immunofluorescent techniques, acts as a marker and enables further study of the CCS-specific expression patterns of HCN4 (hyperpolarization-activated cyclic nucleotide-gated potassium channel 4), connexin, and other membrane proteins. This discovery has improved the understanding of cardiac conduction and confirmed the relevance of specific protein markers such as the various connexins and pacemaker channels. However, further research is necessary to fully uncover the mechanisms of cardiac pacemaking and conduction.

#### **1.4.2. Theories Of Nodal Automaticity**

There are two conflicting theories that have been advanced to explain the mechanism of cardiac activation and nodal automaticity. In short, one theory is the membrane clock (M-clock) hypothesis which states that cardiac automaticity is the result of a combination of voltage generating inward currents potentiated by membrane proteins but is predominately due to hyperpolarization-activated cyclic nucleotide-modulated (HCN) channels. The second theory, the calcium clock (C-cycling) hypothesis, states that the inward current is due to cytosolic cycling of calcium from the SR, and is under subsarcolemmal regulation<sup>40</sup>.

HCN channels are a unique family of ion channels activated upon hyperpolarization in a time-dependent manner and are an integral part of the M-clock theory of nodal automaticity and cardiac activation. An HCN channel is a cation channel that can conduct both  $K^+$  and  $Na^+$  ions. Upon hyperpolarization, the channel is activated by a range of membrane potentials that favor the inward movement of  $Na^+$  down its electrochemical gradient, generating the funny current ( $I_f$ ) which is thought to be responsible for initiating diastolic depolarization (DD) of the membrane towards the threshold potential for rapid depolarization<sup>41</sup>. Voltage clamp experiments have provided insight into the voltage and time dependent relationships between the various membrane currents involved<sup>42</sup>. Subsequently, pacemaker models based on voltage clamp data have successfully produced spontaneous action potentials based on the Hodgkin-Huxley theory of ionic movement, a mathematical model that describes how action potentials are initiated and propagated<sup>43</sup>. These results suggest that a combination of ionic currents, predominately the  $I_f$ , across the sarcolemma constitute the mechanism of cardiac pacemaking<sup>44</sup>.

In the past two decades, another body of research has focused on the effect of cytosolic calcium cycling on automaticity. The current  $Ca^{2+}$ -clock or C-cycling theory posits that the rhythmic release and re-uptake of calcium by the SR activate the inward current ( $I_{NCX}$ ) as a result of the sodium calcium exchanger (NCX), a membrane protein, removing calcium from the subsarcolemmal space. NCX transports three sodium ions for every one calcium ion extruded from the cell<sup>44</sup>, leading to depolarization of the resting membrane during diastole.

In summary, evidence suggests that  $I_f$ , as the pacemaker potential, is activated upon hyperpolarization within the nodal cell's maximum diastolic potential range (-60 mV)<sup>45</sup>.  $I_{NCX}$  is detected during the late diastolic depolarization period prior to the activation of the rapid depolarization L-type calcium current ( $I_{CaL}$ ). Interestingly, the absence of either of these two currents does not fully abolish automaticity but the absence of all other background currents does<sup>45</sup>. Additionally, the actions of membrane channels and exchangers are not only influenced by the electrochemical gradients of ions but also by regulatory factors such as phosphorylation, cyclic AMP (cAMP) levels and protein-protein interactions<sup>40</sup>. Thus, changing the membrane potential during

diastole is complex and the result of an intricate interaction between all current-carrying membrane proteins as well as the subsarcolemmal and intracellular regulatory activities of the automatic nodal cells. Currently, efforts have been focused on merging these two theories of cardiac automaticity and developing a comprehensive pacemaker model which explains all of the observed interactions.

### **1.4.3. Protein Expression And Nodal Differences In Automaticity**

HCN channels are coded for by four genes and are expressed in the heart and throughout the central nervous system. HCN4 channels are strongly and specifically expressed in cells within the nodal regions of hearts across species<sup>35</sup>. In addition to nodal-specific HCN, the NCX protein is also differentially expressed within the nodal regions. While NCX is expressed ubiquitously within the myocardium, there is a higher density of expression within the nodal regions<sup>35</sup>.

In the AVN, the expression profile of these current carrying proteins differs. First, there is a decreased density of HCN expression in the AVN compared to the SAN. Second, as a result of the complex structure of the AVN, HCN expression is heterogeneous within the AVN cell network<sup>34</sup>. Third, immunofluorescent and quantitative PCR studies have arguably shown a higher density of NCX expressed in the AVN in comparison to the rest of the myocardium<sup>35,46</sup>. And four, studies have measured a larger inward NCX current ( $I_{NCX}$ ) in AVN cells than HCN current ( $I_f$ ) particularly during the late diastolic depolarization. The function of HCN within the AVN is further questioned by studies that show a large portion of isolated AVN cells do not display  $I_f$  properties<sup>47</sup>, yet are still spontaneously active. These observations suggest that the inward NCX current, and the underlying subsarcolemmal and intracellular interactions, may play a larger role in pacemaking within the AVN<sup>48</sup>.

Structurally speaking, the AVN is more complex than the SAN. From the endocardial perspective, the AVN can be located between the coronary sinus, the tendon of Todaro and the atrioventricular valve<sup>32</sup>. Additionally, the atrioventricular nodal region also penetrates the central fibrous body across the atrioventricular junction as it develops into the bundle of His and the remaining cardiac conduction fibers. Therefore,

the overall structure of the nodal tract within the AVJ is three dimensional and include portions of the atrium and atrioventricular septal regions (Figure 4)<sup>35</sup>. Furthermore, studies have delimited various sub-regions within the AVJ such as the inferior nodal extension, compact node, penetrating bundle as well as slow and fast pathways leading to this region<sup>34</sup>. However, besides studies on mRNA expressions and immunolabeling of certain functionally relevant proteins, the electrophysiology and functional properties of these specific sub-regions are still largely unknown. Therefore, it can be concluded that, despite similar pacemaking functions within the SAN and AVN regions, the underlying mechanisms of these events are more complex and multi-faceted than originally thought.

## Chapter 2.

### **Thesis Objectives**

Post-operative arrhythmias, such as JET and AVB, occur predominantly in neonates in the pediatric population. They have traditionally been associated with mechanical trauma relating to surgical procedures, but are also closely associated with CPB and other ischemia inducing surgical procedures. We hypothesize that the onset of post-operative arrhythmias is potentiated by the following:

1. The undeveloped nature of the neonatal atrioventricular junction (AVJ) making it particularly susceptible to ischemia reperfusion (I/R) insults.
2. The possible disproportional vulnerability of the neonatal AVJ to a prolonged duration of ischemia compared to a more mature AVJ.
3. Post-operative I/R insults in the neonatal AVJ are exacerbated by the administration of inotropic agonists, increasing the possibility of rhythmic disturbances originating from the AVJ.

In this study, I will examine the variables of age, I/R duration and post ischemia dopamine (DA) administration in a rabbit heart model. The aim is to induce arrhythmias commonly observed post-operatively in the pediatric population under highly controlled experimental settings in healthy hearts and study the effects of each variable. We hypothesize that a combination of young age, ischemic duration and post-ischemia inotropy predisposes the AVJ to dysfunction and, rather than mechanical trauma, are the main factors causing post-operative arrhythmias.

## Chapter 3.

# Experimental Design and Methods

### 3.1. Langendorff Technique

The Langendorff retrograde coronary perfusion technique was developed by Oscar Langendorff in 1895. It is an experimental technique that enables the continuous perfusion of the coronary arteries after the heart has been excised from an animal<sup>49</sup>. To achieve this, a cannula is inserted into the transected aorta and secured with sutures. The opening of this cannula must be placed above the aortic valves to allow the aortic valves to close against the pressure of the perfusate and force the solution through the coronary ostia and into the coronary arterial system.

The perfusate can be delivered via either a constant pressure set up or a constant flow set up. Constant flow perfusion is achieved by setting a constant flow rate, normally with peristaltic pumps, which is comparable to the coronary vascular perfusion rate of the animal studied, in this case, the rabbit. In a constant pressure system, various methods can be employed. The simplest method is using a fluid column set at a fixed height above the cannulated heart. Using gravity, a continuous perfusion at a set pressure is achieved. Additionally, a sealed chamber set up, monitored by a manometer or pressure transducer, can also achieve constant pressure perfusion. Constant pressure and constant flow set ups both have benefits and limitations. In a constant flow system, while the tissue has the potential to receive uniform perfusion, the nature of the system does not allow natural coronary autoregulation to occur. Conversely, while the constant pressure system does allow for autoregulation, uniform perfusion throughout the myocardium is more difficult to achieve. Therefore, the application and design of these systems depends on the specific goals of each study<sup>50</sup> and should be customized with care.

In addition to the choice in perfusion set up, the choice in perfusion solution also warrants consideration. The Langendorff heart is usually perfused with a saline based physiological solution. Typically this is either the standard Tyrode's solution or a Krebs-Henseleit Buffer (KHB) buffer. In addition, studies have also used blood perfusate or perfusate with fatty acids as metabolic substrates instead of glucose or pyruvate. The purpose of saline solutions is to mimic the physiological ionic environment of the plasma and perpetuate a somewhat normal nutrient delivery and ionic environment outside of the body. These saline solutions include varied concentrations of  $\text{Na}^+$ ,  $\text{K}^+$ ,  $\text{Ca}^{2+}$ ,  $\text{Mg}^{2+}$ ,  $\text{Cl}^-$ , and  $\text{PO}_4^{2-}$ , together with glucose and pH buffers.

The solutions vary based on the differences in the concentrations of these ionic salts and the pH buffer used. The choice between the types of perfusate depends on the goals and requirements of each study. For example, suggestions have been made to modify the concentration of specific ions such as  $\text{K}^+$ , and  $\text{Mg}^{2+}$  in studies where the avoidance of arrhythmias is desired<sup>50</sup>. Additionally, pH buffers can also be modified to suit the specific needs of each study. If studies are being designed to observe the function of  $\text{Na}^+/\text{HCO}_3^-$  and  $\text{Na}^+/\text{H}^+$  exchange in pH and metabolic acid-base balance, then the use of a  $\text{CO}_2$  and  $\text{Na}^+/\text{HCO}_3^-$  buffer can be a confounding variable. In these cases, a bicarbonate-free perfusate should be employed. In conclusion, the choice in perfusion solutions and buffering systems should be carefully evaluated prior to beginning the experiment and all aspects of the protocol, from experimental conditions to drug applications, need to be considered.

### **3.2. Optical Mapping Of The Heart**

Cardiac optical mapping (OM) is a technique developed to capture and observe electrical and ionic activities of the heart with high temporal and spatial resolution. Typically, the Langendorff heart is perfused with a potentiometric dye or an ion indicator. The potentiometric or voltage-sensitive dyes used in OM respond rapidly to cardiac changes in membrane potentials, altering their fluorescence emission as a result. Ion indicators, such as Rhod-2AM, are chemical substances that selectively bind to specific ions,  $\text{Ca}^{2+}$  in this case, in the cytosol or various compartments within the cell and are categorized as ratiometric or non-ratiometric. Typically dyes are non-ratiometric when



the quantification of the indicated ionic concentration is directly proportional to the change in the emitted fluorescence intensity. Ratiometric dyes have dual wavelength excitation, such as Fura-2, or dual wavelength emission, such as Indo-1, which means quantifying ion concentration requires the calculation of ratios between the emission intensities at different excitation wavelengths or the intensity ratio between different emissions wavelengths excited at the same wavelength. Ratiometric and non-ratiometric dyes have different excitation and emission spectra depending on whether these indicators are bound or unbound to their target ion. Subsequently, with the right combination of excitation and emission, the emitted fluorescence of both voltage and ion indicators can be captured via a series of still images at a high frame rate<sup>51</sup>, then processed and quantified.

### **3.3. Methods**

#### **3.3.1. Animals**

New Zealand White rabbits were used in this study. The experimental protocols used in this study were approved by the Animal Care Committee of the University of British Columbia, as well as the Animal Welfare Committee of Simon Fraser University. Experiments were also conducted in accordance with the Canadian Council on Animal Care regulations.

#### **3.3.2. Heart Excision**

Ten day old (10-d) and 56 day old (56-d) rabbits were first anaesthetized in an induction chamber with isoflurane at 5 ml/min. Anesthesia was then maintained by a face mask, after being removed from the induction chamber, at 3 ml/min for 10-d rabbits and 4-5 ml/min for 56-d rabbits throughout the excision procedure. Once the animal lost its toe pinch withdrawal reflex, a transabdominal incision was made to expose the diaphragm and the thoracic cavity was opened by cutting the ribcage bilaterally towards the clavicle. The sternum and associated ribs were reflected upwards to expose the heart which was quickly removed and immediately immersed in ice-cold KHB solution. The excised heart was then transferred to the Langendorff set up and the aorta was

swiftly cannulated and secured with a small, blunt artery clip. As the perfusate was free flowing through the cannula prior to cannulation, coronary flow was re-established as soon as the cannula was inserted. Any additional tissue attached to the heart was removed after the cannula was secured with sutures. The ischemic duration of 10-d hearts throughout this initial procedure was approximately 30 seconds; less for 56-d hearts.

### **3.3.3. Whole Heart Optical Mapping Study**

To study the effect of I/R insults on intact immature versus mature rabbit hearts, optical mapping (OM) was employed. Specifically, Langendorff perfused hearts were loaded with the potentiometric dye RH237 (Sigma Aldrich), and motion was stabilized with the myosin ATPase uncoupler Blebbistatin (Tocris). The studied hearts, which were enclosed in custom-built chambers, (Figure 4) were excited at 532 nm and the fluorescence emission (>700 nm) was captured by an Orca Flash 4.0 sCMOS camera (Hamamatsu Photonics) (Figure 4). Analysis of the Regions of Interest (ROI) from the epicardial surface of the hearts was conducted using custom software produced in-lab in the Interactive Data Language (IDL) environment.

### **3.3.4. Solutions**

Excised 10-d (n=38) and 56-d hearts (n=20) were retrogradely perfused via the aorta with KHB buffer (in mM) (118 NaCl, 4.7 KCl, 1.1 MgSO<sub>4</sub>, 1.2 KH<sub>2</sub>PO<sub>4</sub>, 25 NaHCO<sub>3</sub>, 0.1 EDTA, 11 glucose, 2 units of insulin, 2 CaCl<sub>2</sub>, 0.005 ascorbic acid, and pH 7.4, maintained with 95% O<sub>2</sub> and 5% CO<sub>2</sub>) using a constant flow Langendorff set up maintained at 37°C (± 0.5°C). The perfusion rates were 7.5 ml/min for 10-d hearts and 20 ml/min for 56-d hearts.

Additionally, the ischemia mimetic (IM) solution used during the ischemic protocol had the same composition as the KHB buffer with the following modifications (in mM): 6 CaCl<sub>2</sub>, 0 glucose, 5 sodium lactate and 10 MES, pH 6.0. The addition of MES buffer was to ensure appropriate pH buffering at pH 6.0.

### 3.3.5. Exclusion Criteria

Hearts that did not satisfy the following parameters after 10 minutes of perfusion after initial cannulation were excluded from the study:

- a) Heart rate must be between 120 – 250 bpm<sup>52</sup>.
- b) Must be without arrhythmias by the end of the initial perfusion period of 10 min.
- c) Coronaries must be free of any obvious occlusion and clear and expanded after perfusion.
- d) Coronary flow must be 7-8 ml/min in 10-d and 19-21 ml/min in 56-d)<sup>52</sup>.

### 3.3.6. Definitions Of Arrhythmia

To standardize analyses, experimentally-induced arrhythmias were categorized based on discrete quantitative and qualitative parameters. During reperfusion, the following distinct electrical patterns were observed and subsequently allocated into these categories:

1. **Sinus Rhythm** - defined by a 1:1 atrial to ventricular conduction pattern in which the heart rate was not significantly different from the baseline heart rate during initial perfusion or control conditions.
2. **AV Block** - defined by an abnormal atrioventricular conduction pattern, in which the electrical signals from the right atrium were not conducted in a 1:1 manner to the right ventricle. As a result, the frequency of atrial optical action potentials exceeded that of the ventricle (A>V). If the atrial rate was similar to baseline, this was an isolated AVB and categorized the same as in the clinical setting (i.e. first, second degree, third degree).
3. **Sinus Bradycardia** - defined as a sinus rhythm heart rate below the exclusion criteria of normal heart rate range or if it is  $\leq 0.75$  times that of control (A=V).
4. **Sinus Tachycardia** – Sinus rhythm heart rate above the exclusion criteria of normal heart rate range or if it is  $\geq 1.25$  times that of control (A=V) and is independent of the dopaminergic effect.

5. **Tachycardia with VA dissociation (TVAD)** – defined as a ventricular rate that is 1.3 times that of the control and with clear VA dissociation (A<V).

Representative Optical Action Potentials (OPA) of these types of arrhythmias is depicted in Figure 5.

### **3.4. Experimental Protocols**

Once the cannulated hearts reached steady-state conditions and had met the pre-established inclusionary criteria, they were loaded with 0.05-0.1 $\mu$ M RH237 (potentiometric dye) and 13-15  $\mu$ M Blebbistatin. Baseline control data were recorded once motion ceased (Figure 6). Subsequently, the IM solution (in mM: 118 NaCl, 4.7 KCl, 1.1 MgSO<sub>4</sub>, 1.2 KH<sub>2</sub>PO<sub>4</sub>, 6.0 CaCl<sub>2</sub>, 10.0 HEPES, 10.0 MES, 5.0 sodium lactate, 0.0056 ascorbic acid and pH 6.0 maintained with 95% N<sub>2</sub> and 5% CO<sub>2</sub>) was perfused for 15 min. After administration of the IM solution, various ischemic protocols (see Sections 3.4.1 – 3.4.3) were applied. During the reperfusion phase, DA was applied to the perfusate and data were collected at 5 min intervals during the reperfusion phase.

#### **3.4.1. Study 1: Effect Of Experimental Procedures On Cardiac Performance**

To study the natural decay of cardiac rhythm due to experimental conditions, 10-d and 56-d hearts (n=3, 3, respectively) were perfused and monitored for 2 hours prior to the addition of DA (+DA). Hearts were loaded with the potentiometric dye RH 237 and motion stabilized with Blebbistatin. Data were recorded first, after the initial stabilization period and then again, after 2 hours of perfusion. After DA was added, data were acquired every 5 min for 30 min.

#### **3.4.2. Study 2: Effect Of Age On Reperfusion Arrhythmias**

The I/R protocols were applied to two age groups. 10-d rabbits were used to mimic the neonate age and 56-d rabbits were used to mimic the mature age group. New Zealand White rabbits reach sexual maturity by 56-d.

### **3.4.3. Study 3: Effect Of Post Ischemia DA Administration**

In order to observe the effect of post-ischemic administration of DA, two sets of experiments were conducted. Hearts were either perfused after 30 min GI with (+ DA) 20  $\mu$ M DA or without (- DA) 20  $\mu$ M DA.

### **3.4.4. Study 4: Effect Of Ischemic Duration On Reperfusion Arrhythmias**

After perfusion with the IM solution, the hearts were placed under zero-flow, normothermic (normal body temperature, 38.3-39.4<sup>0</sup>C for rabbits), global ischemia (GI) for either 30 (Protocol 1) or 90 (Protocol 2) min to induce ischemic insults. Immediately after GI, the hearts were perfused with KHB solution plus 20  $\mu$ M DA for 15 – 30 min. Figure 7 illustrates the timelines of these two protocols.

## **3.5. Analysis**

Optical Action Potential (OPA) analysis was conducted using custom software written in-lab. Post-acquisition analysis, including de-trending, normalization and filtering, were conducted utilizing this software. Paired t-tests were conducted to detect differences between the mean heart rates before and after each protocol, as well as the difference between the mean chamber rates at specific acquisition times. An  $X^2$  test of independence was applied to evaluate the significance of age as a categorical variable and its effect on reperfusion arrhythmias frequency. Additionally, McNemar's test was applied where appropriate to determine the differences between the correlated proportions of the sample population with and without arrhythmias, before and after the application of various protocols. Differences were considered statistically significant at  $p < 0.05$ .

## Chapter 4.

### Results

Under control conditions, the rabbit hearts did not develop rhythmic abnormalities when perfused continuously with KHB buffer for 2 hours (Figure 8). The effect of DA was immediate and persistent, with an average 1.3-fold increase in heart rate for at least 30 min following administration (Table 1). In comparison, I/R Study 2 (GI for 30 min) and 4 (GI for 90 min) both induced abnormal atrioventricular synchrony and cardiac rhythmicity upon reperfusion in 10-d hearts. In 56-d hearts, only Study 4 induced abnormal rhythms upon reperfusion.

#### **4.1. I/R Induced Arrhythmias Were Dependent On Maturation Stage**

##### **4.1.1. 10-d (Neonate) - Reperfusion Time (5 Min)**

Of the rabbit hearts studied, 33% exhibited tachycardia with VA dissociation (TVAD), 34% exhibited AVB, and 25% exhibited bradycardia.

The mean resting heart rate in the TVAD group was  $208 \pm 20$  bpm, the mean reperfusion atrial rate was  $126 \pm 53$  bpm and the mean ventricular rate was  $215 \pm 53$  bpm. There was no significant difference between the mean reperfusion atrial rate and ventricular rate versus control heart rate ( $p > 0.05$ ). However, there was a difference between mean atrial and ventricular rate at 5 min into reperfusion ( $p < 0.05$ ).

In the AVB group, the mean control heart rate was  $211 \pm 34$  bpm, the average reperfusion atrial rate was  $103 \pm 75$  bpm and the average reperfusion ventricular rate was  $32 \pm 43$  bpm. There was significant statistical difference between the mean atrial

and ventricular rates before and after ischemia, as well as between the mean atrial and mean ventricular rates at 5 min into the reperfusion phase ( $p < 0.05$ ). This indicates that not only did these hearts display AVB but did not recover and resume a normal heart rate within the experimental time frame.

The bradycardia group yielded an average reperfusion heart rate of  $72 \pm 25$  bpm, significantly lower than the control heart rate of  $192 \pm 7$  bpm ( $p < 0.05$ ).

#### **4.1.2. 10-d (Neonate) - Reperfusion Time (10 Min)**

At 10 min into reperfusion, 33% of the 10-d hearts experienced AVB and 8% experienced TVAD (Figure 9).

The AVB group had an average control heart rate of  $197 \pm 22$  bpm while the reperfusion atrial rate was  $217 \pm 22$  bpm and the reperfusion ventricular rate was  $113 \pm 82$  bpm. The reperfusion atrial rate and ventricular rates were not significantly different from the resting heart rate ( $p > 0.05$ ); however, there was significant difference between the atrial and ventricular rates ( $p < 0.05$ ).

In the TVAD category, 1 out of 12 hearts experienced AV dissociation at 10 min into reperfusion. The control heart rate was 231 bpm, reperfusion atrial rate was 286 bpm and reperfusion ventricular rate was 300 bpm.

#### **4.1.3. 56-d (Mature) – Reperfusion Time (5, 10 Min)**

As opposed to the neonate hearts, 100% of the mature 56-d hearts in study 2 recovered back to sinus rhythm within 5 min into reperfusion (Figure 9). 56-d rabbits did not display any aberrant electrical activities upon reperfusion after 30 min GI.

Chi-square ( $X^2$ ) tests of independence indicate that, after 30 min GI, there was a significant difference in the proportions of arrhythmia between the two age groups. This suggests that the reperfusion arrhythmias that occurred at 5 min and 10 min into reperfusion were age-dependent. ( $X^2 = 5.33$ ,  $p < 0.05$ ;  $X^2 = 4.14$ ,  $p < 0.05$  for 5 and 10 min, respectively). Table 2 shows the heart rate data for all the test subjects under Study 2.

## **4.2. Post Ischemic Administration Of DA Did Not Influence I/R Induced Arrhythmias**

Hearts reperfused with and without DA had a similar course of post-ischemic recovery and developed similar arrhythmias. 10-d hearts reperfused with DA seemed to have longer lasting arrhythmias; however, there was not a clear trend in the study group. In 56-d hearts reperfused without DA; expectedly, there was a fraction of hearts (60% at 5 min reperfusion, 20% at 10 min reperfusion) that experienced bradycardia, while all 56-d hearts perfused with DA recovered in sinus rhythm. (Figure 10) Table 3 shows the heart rates for all study subjects under Study 3.

## **4.3. Increased I/R Duration Exacerbate Arrhythmias To A Greater Degree In Neonate Hearts Than In Mature Hearts**

To determine the effect of ischemia duration on reperfusion arrhythmias, study 4 was conducted wherein the hearts were subjected to 90 min GI, followed by 15 min of perfusion with the IM solution. Neonate hearts were found to experience a disproportionate increase in the severity of reperfusion arrhythmias compared to the hearts from the 56-d rabbits.

### **4.3.1. 90 min GI, 10-d (Neonate)**

None of the hearts (n=6) in the neonate group recovered ventricular rhythm until 15 min into the reperfusion phase (Figure 9, right panel), leaving the hearts in a persistent complete conduction block. The atria, unlike the ventricles, were able to recover quickly upon reperfusion with an average OPA rate of  $170 \pm 55$  bpm;  $0.86 \pm 0.24$  times that of the control rate. This is consistent with the rate of rhythmic decay observed in the control group (Figure 8). Furthermore, only one neonate heart achieved AV synchrony after 30 min of continuous reperfusion with DA while the other 5 hearts continued to exhibit some form of AVB throughout the reperfusion phase.



#### **4.3.2. 90 min GI, 56-d (Mature)**

In contrast, all 56-d hearts (n=6) recovered sinus rhythm by 15 min of reperfusion and did not display any reperfusion arrhythmias beyond this time. However, some abnormal rhythms were observed as a result of Protocol 2 within the first 10 min of reperfusion (Figure 9). 50% of the hearts in this group recovered AV synchrony within 5 min of reperfusion. One heart was bradycardic (reperfusion: 97 bpm; baseline: 182 bpm) and 2 out of the 6 hearts displayed TVAD between 5 – 10 min into reperfusion (Fig. 9). All hearts recovered sinus rhythm by 15 min of reperfusion.

Table 4 shows the heart rate data for all test subjects under Study 4.

#### **4.4. Summary Of Results**

In total, 12 10-d (neonate) hearts and 4 56-d (mature) hearts were studied in Study 2 (30 min GI). 92% of the neonate hearts developed arrhythmias 5 min into the reperfusion phase and 42% of these hearts continued to exhibit some form of arrhythmia 10 min into reperfusion. 100% of the 56-d hearts in Study 2 recovered normal sinus rhythm and no arrhythmias were observed. For Study 4 (90 min GI), 6 10-d hearts and 6 56-d hearts were studied. During reperfusion, 100% of the neonate hearts experienced sustained arrhythmias lasting the entire 30 min of reperfusion. In contrast, only 50% of the 56-d hearts experienced some form of arrhythmia at 5 min into reperfusion and by 15 min of reperfusion, all 56-d hearts had recovered sinus rhythm.

## Chapter 5.

### **Discussion**

#### **5.1. Methodology**

##### **5.1.1. Animal Models**

While animal models are very useful tools to broaden our understanding of physiological responses to pathology, there are intrinsic differences between humans and other mammals that need to be addressed. In general, organ systems and tissues tend to have similar macroscopic functions across mammalian species; however, other aspects such as relative body size and variations in gene sequences and expression can be quite different. In cardiac research, mice, rats and rabbits are frequently used for their small size, their relatively low cost, ease of breeding and maintenance, while canine, porcine or bovine hearts may be used for functional studies where mimicking the human cardiac workload is desired. Choosing the appropriate animal for study is an important step in the design of the study and experimental set up. While smaller hearts are easier to work with when studying single cell isolation or OM, larger hearts are more appropriate when multiple instruments are needed to monitor various cardiac parameters simultaneously. Additionally, when studying electrophysiology and arrhythmias, cross species variation in cardiac electrophysiology should be considered.

For this study, the rabbit heart was chosen as the animal model. First, the rabbit's cardiac action potential is much closer to the human cardiac action potential than mouse and other murine models. Second, the physical parameters of the OM equipment imposed restrictions on the size of the heart or heart wedges that were to be studied, making the rabbit the most appropriate animal. And third, the conduction axis in 10-d and 56-d rabbit hearts had been previously mapped in the lab.

### **5.1.2. Langendorff Retrograde Perfusion Technique**

Using the Langendorff technique to conduct *ex-vivo* cardiac studies offers both advantages and disadvantages. This technique allows researchers to conduct experiments such as I/R, stimulation protocols, functional studies and pharmaceutical studies on hearts in isolation and while animals are sacrificed, there is no long term suffering as there would be in live animal experiments. Additionally, these studies allow the investigator to better control variables such as blood coagulation causing unwanted ischemia and unknown or uncontrolled systemic responses to experimental protocols. With a wide range of animal models, researchers can gain insight into the similarities and differences in their physiological functions. This knowledge can inform applications to alleviate human pathology.

However, there are also disadvantages to the Langendorff model. Intrinsic to *ex-vivo* studies, the excised organ is continuously deteriorating during the course of the study. Consequently, it is imperative to understand the rate of this decay and account for this in the interpretation of any results to avoid introducing confounding effects. Perfusion parameters such as constant flow or constant pressure, as discussed previously in the Introduction section, can also impact experiments negatively when used inappropriately. While studying the heart in isolation to understand cardiac physiology is informative, it is by definition not integrated into its functional cardiovascular system and results must be applied with caution. In isolation, Langendorff hearts lack the contractile resistance *in vivo* hearts normally experience with afterload and the autonomic nervous systems' intrinsic nervous regulation is absent.

### **5.1.3. Optical Mapping Of The Rabbit Heart**

Various challenges were encountered during the initial phase of this study in the development of optical mapping technology and in its application to the rabbit heart. While the technology of the optical mapping was largely prepared by Dr. Lin, from our lab, I was responsible for building the experimental chambers, designing the perfusion set up and subsequently troubleshooting the experimental protocols. The optical mapping chamber was designed using Solidworks (USA) and several requirements or parameters required careful consideration. Firstly, the chamber size need to be

appropriate for the hearts studied. Since we used hearts at various developmental stages the relative dimensions of the optical mapping chamber also needed to change. Secondly, the constant flow of solution through the chamber can create practical problems during experimentation. In order to protect the electronic equipment in the vicinity and to prevent any movement of the fluid meniscus from affecting image acquisition, fluid from the heart chamber was allowed to flow into a secondary overflow chamber from which solution was suctioned and recirculated. Lastly the optical mapping chamber required two sides to be transparent allowing image acquisition. Figure 11 shows the computer assisted design of the optical chamber. When designing the perfusion set up minimizing the volume of solution within the perfusion lines was very important. This is to ensure we minimize the use of certain chemicals that was necessary for each protocol and to ensure thermoregulation of the solution prior to the heart was within the accepted normal range. Finally, various concentrations of the motion stabilizer Blebbistatin and potentiometric dye RH 237 was also tested to ensure the heart was void of motion artifacts and photo bleaching of the dye was kept at a minimum.

## **5.2. Reperfusion Arrhythmias**

This is a novel experimental study designed to reproduce the impact of three prominent risk factors implicated in the development of post-operative arrhythmias: age, duration of CPB and post-operative administration of inotropic agents, in this case, DA. Consistent with single cell data, these conditions also produced AVB in some hearts, confirming that insult to the AVN can be produced in the absence of mechanical trauma. In clinical settings, accelerated rhythms with VA or AV dissociation can co-exist with conduction blocks,<sup>53</sup> as was observed in this study. The healthy cardiac conduction axis in the neonate was found to be sensitive to extreme pH (6.0), calcium overload (6 mM), and prolonged ischemic duration (30-90min). By manipulating the ischemic conditions and duration, we were able to experimentally produce a model for post-operative arrhythmias observed in infants.

This approach allowed direct observation of the impact of I/R insults on age- and tissue-specific cardiac pacemakers, as seen in the changes to cardiac conduction that

are arrhythmogenic during the reperfusion phase. Exposure to an IM solution prior to GI in whole heart OM was key to inducing the observed reperfusion injuries, suggesting that the hypercalcemic and low pH IM solution was an influential factor. GI for 30 min without IM solution did not induce arrhythmic responses in neonates (Table 4). Mechanistically, the altered extracellular calcium environment and pH are most likely involved but due to the inherent complexity of cellular machinery and regulation, firm conclusions cannot currently be made.

Automaticity in nodal cells is integrally related to calcium handling and cycling<sup>45,48</sup>. Calcium efflux, a result of oscillatory cytosolic calcium activity, is driven by the influx of Na<sup>+</sup> ions via the sodium-calcium exchanger (NCX), late in phase 4 of the nodal action potential<sup>45</sup>. In the nodal regions, transmembrane calcium transients play important roles in eliciting diastolic depolarization which potentiate spontaneous action potentials and regulate cytosolic calcium cycling. Aside from the effect of altered calcium handling, experimental changes to ionic and pH balance are also detrimental to cardiac metabolism, mimicking the effects of hypoxia. Introducing calcium and pH changes prior to ischemia may induce disproportionate disturbances to the neonate AV conduction path, causing abnormal function and arrhythmogenesis. Studies have shown that chronic levels of hypoxia can cause cardiac metabolism to rely more on anaerobic ATP production which, in turn, increases anaerobic by-products. It is known that calcium handling and the outcome of I/R insult in cardiomyocytes are heavily influenced by changes in metabolic by-products such as lactate, ADP/ATP ratio and pH<sup>54</sup>. Interestingly, in previously conducted single cell experiments not reported here, only immature AVN cells were affected by I/R, in comparison to SAN cells and mature AVN cells, displaying aberrant electrical and calcium activity. The findings of this study are consistent with the literature and support the hypothesis that I/R insults disproportionately disrupt the immature AVN and can be arrhythmogenic.

There are three important limitations to this study. First, it is intrinsically challenging to relate experimental phenomenon to clinical observations and diagnoses. Among the arrhythmias, while some correlations can be easily drawn between experimental results and clinical observations, such as for sinus bradycardia and tachycardia, other correlations for variations of AVB and VA dissociative arrhythmias are harder to identify. Second, it is difficult to differentiate SVT from JET, even though the

existence of AV conduction abnormalities in the rabbit model suggest the observed TVAD is likely JET. In order to observe these reperfusion arrhythmias with a higher level of discrimination, an endocardial preparation that is able to withstand hours of experimentation and a more detailed optical mapping study is necessary. Third, the cellular mechanisms of I/R induced arrhythmias are difficult to discern. Although it can be indirectly shown that calcium handling and pH in combination with ischemic duration may influence reperfusion arrhythmias, a mechanistic explanation of why these arrhythmias occur cannot yet be provided. However, we have developed a method with which arrhythmias commonly observed post-operatively can be induced experimentally without any surgical trauma to the conduction axis in normal, healthy rabbit hearts. This extends the possibility of developing alternative etiologies and enables further exploration of specific substrates for, and mechanisms of, these arrhythmias.

### **5.2.1. Ionic Basis Of Ischemia Reperfusion**

Ischemia and the subsequent re-establishment of flow, known as reperfusion, can severely impact the viability of a cell, affecting multiple cellular compartments and processes, among which is the accumulation of metabolites within and surrounding the cell. The effect of I/R on cardiac myocytes is paradoxical because reperfusion does not to alleviate the damage sustained during ischemia but instead exacerbates it. This is the result of systemic failures in cellular metabolism, regulation and ionic balance. Failure to regulate metabolic waste and regain pH balance can trigger a cascade of ionic imbalances that potentiates arrhythmias and cell damage. Additionally, metabolic stress and subsequent re-oxygenation can trigger the production of reactive oxygen species which further disrupts the cellular machinery and damages cellular structures. Finally, the combination of metabolic stress accompanied by pH and ionic imbalances can trigger the mitochondria to initiate cell apoptosis or potentiate arrhythmias<sup>55,56</sup>.

Cardiac tissue is particularly sensitive to ischemia since myocytes rely heavily on oxidative phosphorylation and the electron transport chain to produce ATP. With a decrease in oxygen delivery, ATP production begins to rely on anaerobic mechanisms.

Acidosis affects the cell in a number of ways. In rabbit AVN cells, acidosis has been shown to inhibit L-type calcium current and delayed rectifier potassium currents<sup>57</sup>. It can also cause a decrease in myocyte contractility as a result of decreased myofilament calcium sensitivity despite elevated levels of systolic and diastolic cytosolic calcium<sup>58,59</sup>. The elevated levels of calcium observed during I/R are largely due to the reversal of the NCX current as part of the cells' effort to regain pH balance<sup>60</sup> and NCX inhibition has been shown to alleviate these effects<sup>61</sup>. Elevated levels of calcium can affect SR function since the SR functions to remove calcium from the cytosolic space. Increased levels of cytosolic calcium can lead to SR calcium overload, which has been shown to be arrhythmogenic<sup>60,62</sup>. Along with promoting arrhythmogenesis, calcium oscillations during the reperfusion phase can also cause hypercontracture in cardiomyocytes which can further deplete ATP storage and contribute to myocyte death<sup>60</sup>.

What determines the cell's ability to survive the reperfusion phase appears to depend on two factors: first, how the myocytes handle this calcium-overload and second, how the mitochondria respond. Accumulation of cytosolic calcium not only induces SR overload but also stimulates mitochondrial  $\text{Ca}^{2+}$  overload, which is exacerbated by independently occurring mitochondrial calcium accumulation, critically affecting the mitochondrial machinery. Mitochondrial ability to regain metabolic and ionic control has been linked to the rate and quality of myocardial recovery from I/R<sup>55,63,64</sup>. As well, sustained calcium and calmodulin interaction elevates calmodulin-dependent protein kinase II (CaMKII) activity. This kinase targets a number of proteins that mediate the effect of I/R; for example, activated CaMKII can increase SR  $\text{Ca}^{2+}$  ATPase (SERCA2a) activity through phosphorylation of phospholamban, may increase RyR2 *Po* and alter other ion channel dynamics<sup>65</sup>. Calcium mediated CaMKII activity is an important mediator of I/R injury in ischemic heart diseases<sup>66,67</sup>.

## **5.3. Future Directions**

### **5.3.1. Dual Optical Mapping**

OM is an immensely useful tool for the study of surface electrophysiology and to visualize cardiac electrophysiology on the tissue and organ level. In this study, a voltage-

sensitive dye was used to visualize electrical activities; however, it is also possible to visualize calcium transients using calcium indicators. Dual OM is a technique that investigators employ to observe the interplay between electrical currents and calcium transients, typically achieved by using two different sensors and then matching the captured frames temporally to observe simultaneous events. We have developed a technique whereby both emissions are captured simultaneously by the same sensor. The challenge with implementing our dual OM technique is that with extremely sensitive cameras, such as the Orca Flash 4, signal bleed-through between the voltage and calcium sides of the frame can significantly affect the results. Current attempts at dual OM in the rabbit whole heart set up have shown that approximately one third of the fluorescent intensities captured on the calcium side of the sensor are actually voltage signals. This ratio is significantly larger than the expected 10% bleed-through experienced in other models of dual OM. Further refinement of this technique is ongoing.

Along with resolving the problem of signal bleed-through, another aspect of OM that requires further development is the ability to obtain high temporal resolution while maintaining a high level of spatial resolution and a wide field of view in order to capture the whole epicardial surface. In this study, OM recordings were captured at 100 frames per second (fps). This is the lowest temporal setting for the Orca Flash 4 camera. A typical rabbit cardiac action potential recorded in our experiments is between 240 to 400 ms long. At the rate of 100 fps, each frame is 10 ms in duration, with each action potential recorded in 20 to 40 frames; however, this level of temporal resolution may be inadequate when considering the changing dynamics of cardiac arrhythmias and the specific events which govern each action potential. Events such as diastolic depolarization, peak of depolarization and transient outward currents all affect the shape of the action potential and, under some circumstances, need to be captured with high fidelity. However, there is a tradeoff to consider if the frame rate is simply increased - there are fewer photons emitted in that interval which may seriously reduce the S/N ratio. Current studies have used settings as low as 100 x 100 pixels of spatial resolution to map whole hearts<sup>68</sup>. Considering the sensor used in this study, which possesses an effective screen size of 13 mm x 13 mm, a resolution of 100 x 100 pixels would be equivalent to an effective pixel size of 130  $\mu\text{m}$  x 130  $\mu\text{m}$ . Additionally, post-acquisition binning of pixels to remove motion artifacts and noise is usually conducted so the



effective size of each pixel is expanded further. If this effective pixel size is compared to the typical myocyte size, it is clear that this level of spatial resolution is not sufficient to observe electrical activities within specific regions of the heart, such as the AVN or conduction axis, or epicardial aberrant electrical events that are restricted to certain ectopic foci. Therefore, further refinement of spatial and temporal resolution, as well as increasing the ability to reliably analyze these complex matrices of data, is warranted.

### **5.3.2. Endocardial Mapping**

In order to observe the CCS and study the mechanisms of I/R induced insults in the AVN, developing an endocardial OM technique would be very useful. This technique would enable direct observation of the AVN during ischemia and subsequent reperfusion, allowing study of aberrant electrical and ionic activities at the tissue level. The challenge with this technique is maintaining the viability of the rabbit heart throughout an extensive I/R protocol. Unlike mouse hearts, rabbit tissue is thicker and cannot withstand being simply superfused during the entire experimental procedure. The development of a perfusion system that is able to sustain rabbit myocardial health for an extended period of time would be instrumental to the success of rabbit endocardial OM.

## Chapter 6.

### **Conclusion**

In this study, we developed a novel experimental design to study the effect of three primary risk factors for post-operative arrhythmias in intact rabbit hearts. We tested the hypothesis that post-operative arrhythmias are related to I/R. Our results show that I/R protocols can produce arrhythmias similar to those observed in pediatric patients post cardiac corrective surgeries. Additionally, pre-ischemia alterations of the ionic environment seem to play a role in exacerbating the effect of GI. We have shown clearly that reperfusion arrhythmias are age- and I/R duration dependent. Specifically, young age and prolonged ischemic durations tend to worsen reperfusion arrhythmias. We propose that the complex heterogeneous structure and function of the AV conduction axis in combination with young age is particularly susceptible to I/R injuries. We conclude that surgical conditions that expose neonate pediatric patients to prolonged ischemia contribute to the occurrence of post-operative arrhythmias. Furthermore, pre-existing alterations to cardiac metabolism, potentially the result of pre-existing hypoxia mimicked by our IM perfusate, may increase the likelihood of reperfusion arrhythmias. Together our cellular pacemaker model (previously studied<sup>27</sup>, data not shown here) and whole heart OM model provide the framework for generating testable hypotheses at the cellular, molecular and tissue level to further our knowledge of arrhythmias in post cardiac surgery neonates.

**Table 1: Study 1 control experiments (hearts perfused for 2 hours continuously, (+) 20  $\mu$ M DA)**

Control	Sinus Rhythm			Bradycardia			AV Block			TVAD		
	10-d						56-d					
	Baseline		Perf- 120 min		(+ DA 5 min		Perf- 120 min		(+ DA 5 min		(+ DA 10 min	
HR (bpm)												
N	A	V	A	V	A	V	A	V	A	V	A	V
1	207	207	222	222	286	286	182	186	186	300	286	286
2	250	250	207	207	300	300	176	171	171	286	316	316
3	240	240	200	200	300	300	182	182	182	316	300	300
<b>Average</b>	<b>232</b>	<b>232</b>	<b>210</b>	<b>210</b>	<b>295</b>	<b>295</b>	<b>180</b>	<b>180</b>	<b>180</b>	<b>301</b>	<b>301</b>	<b>301</b>
<b>STDEV</b>	<b>23</b>	<b>23</b>	<b>11</b>	<b>11</b>	<b>8</b>	<b>8</b>	<b>3</b>	<b>8</b>	<b>8</b>	<b>15</b>	<b>15</b>	<b>15</b>

**Table 2: Study 2 (30 min GI, reperfusion, (+) 20 μM DA)**

HR (bpm) N	Sinus Rhythm			10-d Bradycardia			56-d AV Block			TVAD		
	Baseline		R 5 min		R 10 min		Baseline		R 5 min		R 10 min	
	A	V	A	V	A	V	A	V	A	V	A	V
1	188	188	84	84	261	261	120	120	102	102	128	128
2	167	167	96	0	240	150	140	140	113	113	140	140
3	200	200	84	204	261	261	130	130	125	125	120	120
4	187	187	36	36	200	200	176	176	107	107	150	150
5	200	200	72	72	182	182						
6	214	214	0	0	192	0						
7	231	231	108	168	286	300						
8	214	214	150	91	207	111						
9	194	194	186	273	231	192						
10	250	250	167	36	288	288						
11	214	214	214	214	273	273						
12	250	250	216	276	273	273						
<b>Average</b>	<b>209</b>	<b>209</b>	<b>118</b>	<b>121</b>	<b>241</b>	<b>208</b>	<b>142</b>	<b>142</b>	<b>112</b>	<b>112</b>	<b>135</b>	<b>135</b>
<b>STDEV</b>	<b>25</b>	<b>25</b>	<b>69</b>	<b>101</b>	<b>38</b>	<b>88</b>	<b>24</b>	<b>24</b>	<b>10</b>	<b>10</b>	<b>13</b>	<b>13</b>

**Table 3: Study 3 (30 min GI, reperfusion, (-) DA)**

HR (bpm) N	Sinus Rhythm			Bradycardia			Sinus Tachycardia			AV Block			TVAD			
	10-d			56-d			56-d			56-d			56-d			
	Baseline A	Baseline V	Baseline V	R 5 min A	R 5 min v	R 5 min v	R 10 min A	R 10 min V	R 10 min V	Baseline HR A	Baseline HR V	Baseline HR V	R 5 min A	R 5 min v	R 5 min v	R 10 min A
1	180	180	180	180	480	180	180	180	192	192	192	84	84	84	120	120
2	214	214	240	240	240	250	250	250	144	144	144	84	84	84	108	108
3	158	158	132	132	132	180	180	180	143	143	143	36	36	36	84	84
4	162	162	120	120	480	132	132	132	171	171	171	108	108	108	125	125
5	180	180	96	96	564	144	144	144	168	168	168	24	24	24	78	78
6	180	180	72	72	72	168	168	168	168	168	168	132	132	132	144	144
7	220	220	36	36	36	156	156	156	180	180	180	108	108	108	138	138
8	192	192	72	72	24	132	132	132	154	154	154	118	118	118	136	136
9	144	144	12	12	0	120	120	0	150	150	150	96	96	96	139	139
10	156	156	72	72	36	132	132	132	146	146	146	129	129	129	130	130
11	168	168	0	0	0	150	150	0								
12	180	180	36	36	12	138	138	138								
13	168	168	120	120	0	144	144	144								
14	156	156	36	36	48	120	120	60								
15	156	156	63	63	63	128	128	128								
16	156	156	180	180	60	132	132	132								
17	156	156	24	24	182	111	111	111								
18	168	168	0	0	0	138	138	138								
19	150	150	60	60	24	144	144	72								
20	168	168	120	120	408	150	150	150								
<b>Average</b>	<b>171</b>	<b>171</b>	<b>85</b>	<b>143</b>	<b>187</b>	<b>147</b>	<b>127</b>	<b>58</b>	<b>162</b>	<b>162</b>	<b>162</b>	<b>92</b>	<b>92</b>	<b>92</b>	<b>120</b>	<b>120</b>
<b>STDEV</b>	<b>20</b>	<b>20</b>	<b>65</b>	<b>187</b>	<b>187</b>	<b>30</b>	<b>58</b>	<b>58</b>	<b>17</b>	<b>17</b>	<b>17</b>	<b>37</b>	<b>37</b>	<b>37</b>	<b>23</b>	<b>23</b>

**Table 4: Study 4 (90 min GI, reperfusion, (+) 20 μM DA)**

		Sinus Rhythm						Bradycardia						AV Block						TVAD					
		10-d						56-d																	
HR (bpm)	N	Baseline		R 5 min		R 10 min		Baseline HR		R 5 min		R 10 min		Baseline HR		R 5 min		R 10 min							
		A	V	A	V	A	V	A	V	A	V	A	V	A	V	A	V	A	V						
1		207	207	128	0	231	0	182	182	97	97	128	128	182	182	97	97	128	128						
2		214	214	251	0	214	0	158	158	136	136	171	171	158	158	136	136	171	171						
3		194	194	144	0	144	0	182	182	136	136	176	176	182	182	136	136	176	176						
4		174	174	156	0	132	0	188	188	182	857	207	207	188	188	182	857	207	207						
5		188	188	240	0	240	0	167	167	143	143	182	182	167	167	143	143	182	182						
6		210	210	192	12	228	60	182	182	207	500	273	273	182	182	207	500	273	273						
<b>Average</b>		<b>198</b>	<b>198</b>	<b>185</b>	<b>2</b>	<b>198</b>	<b>10</b>	<b>177</b>	<b>177</b>	<b>150</b>	<b>312</b>	<b>190</b>	<b>190</b>	<b>177</b>	<b>177</b>	<b>150</b>	<b>312</b>	<b>190</b>	<b>269</b>						
<b>STDEV</b>		<b>15</b>	<b>15</b>	<b>51</b>	<b>5</b>	<b>47</b>	<b>24</b>	<b>11</b>	<b>11</b>	<b>39</b>	<b>306</b>	<b>48</b>	<b>48</b>	<b>11</b>	<b>11</b>	<b>39</b>	<b>306</b>	<b>48</b>	<b>237</b>						

**Table 5: 10-d control experiment (no IM, 30 min GI, reperfusion with KHB)**

HR (bpm)	Sinus Rhythm		Bradycardia		AVB		TVAD	
	Baseline				R 5 min		R 10 min	
N	A	V	A	V	A	V	A	V
1	156	156	154	154	156	156	156	156
2	222	222	162	162	182	182	182	182
3	231	231	214	214	214	214	214	214
<b>Average</b>	<b>203</b>	<b>203</b>	<b>177</b>	<b>177</b>	<b>184</b>	<b>177</b>	<b>184</b>	<b>184</b>
<b>STDEV</b>	<b>41</b>	<b>41</b>	<b>33</b>	<b>33</b>	<b>29</b>	<b>33</b>	<b>29</b>	<b>29</b>

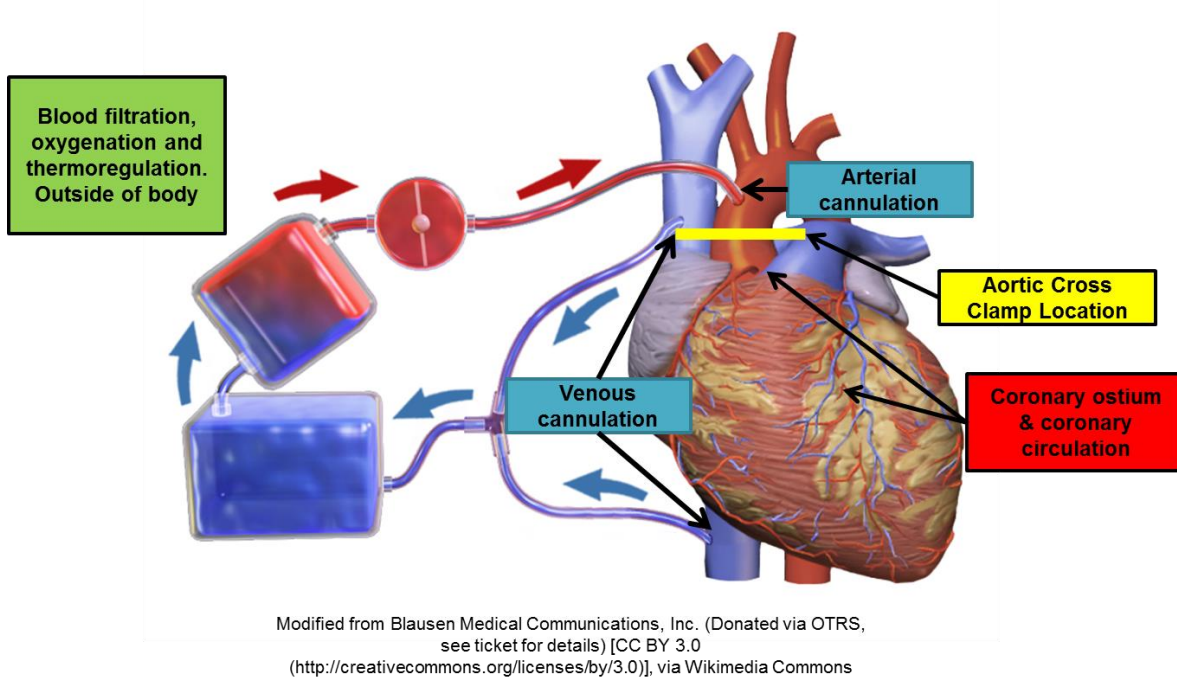
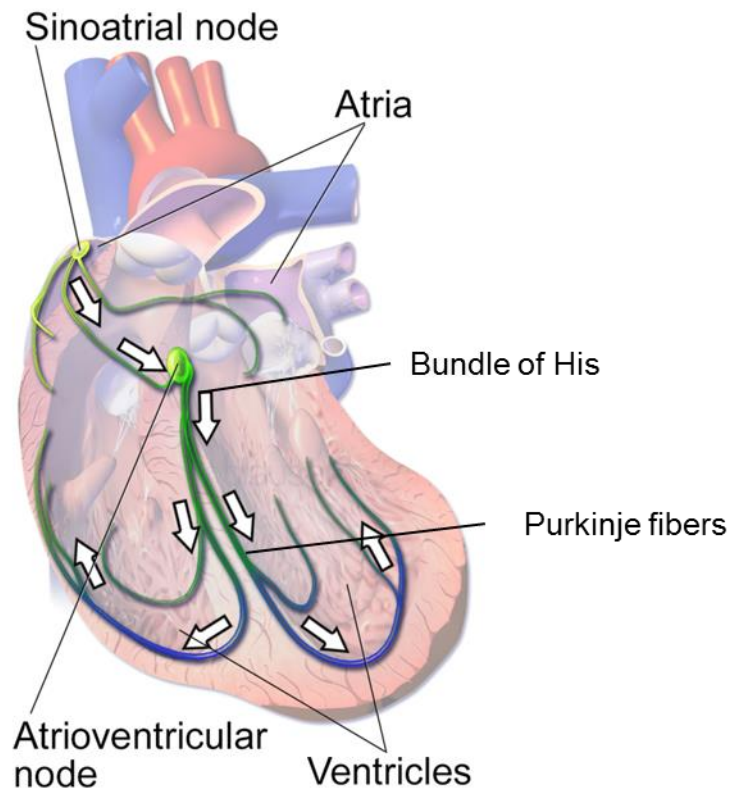


**Figure 1: Cardiopulmonary bypass schematic**

Blood is drained from the body via the venous cannulation and processed outside of the body. After blood is re-oxygenated, temperature controlled and filtered, it is pumped back into the body via the arterial cannulation.





Modified from Blausen Medical Communications, Inc. (Donated via OTRS, see ticket for details) [CC BY 3.0 (<http://creativecommons.org/licenses/by/3.0>)], via Wikimedia Commons

**Figure 2: Cardiac conduction axis**

Automatic pacemaking occurs at the sinoatrial node. Signal is conducted through the atria to the atrioventricular node and passed along to the conduction fibers within the ventricular septum.

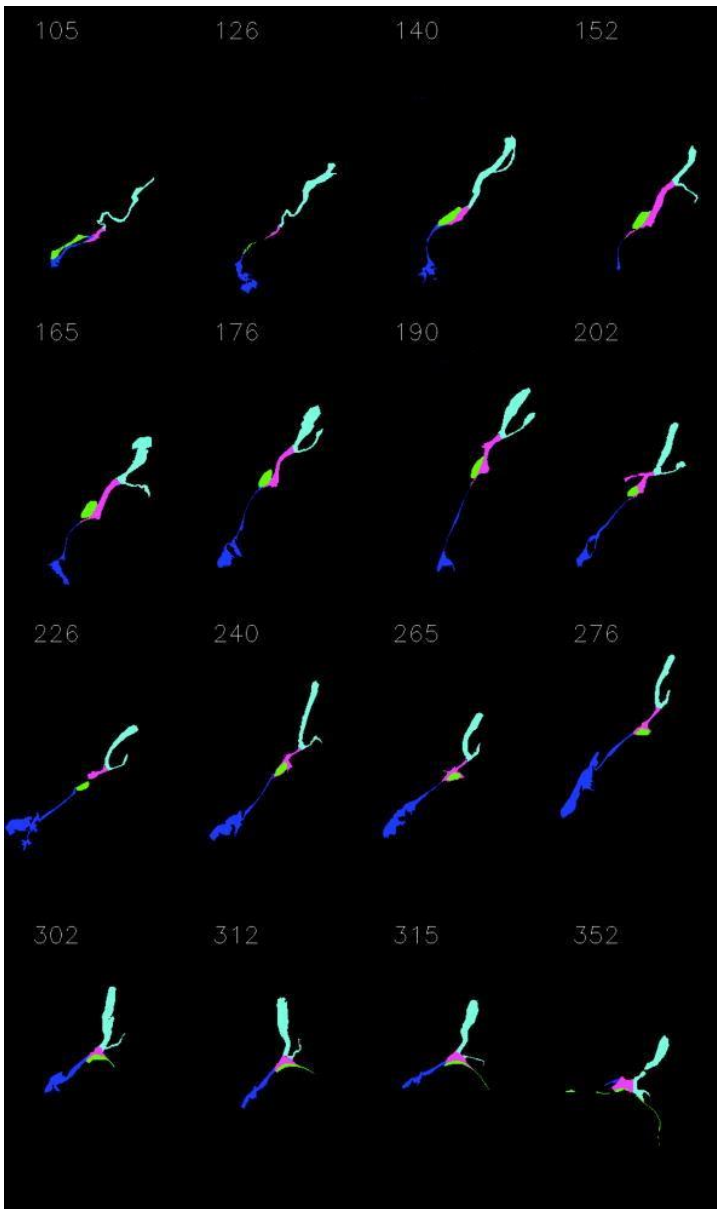


**Figure 3: Location of AVN pacemakers within the AVJ**

Cartoon outline of structures of the atrioventricular junction are detected using Masson's trichrome and immunohistochemistry. The areas coloured include: nodal track (green), aorta and aortic valve (cyan blue), tricuspid valve (navy blue), and the central fibrous body (fusia). Sections are 10  $\mu\text{m}$  thick and span the region between section 105 and 352, which is approximately 2 mm thick in total.

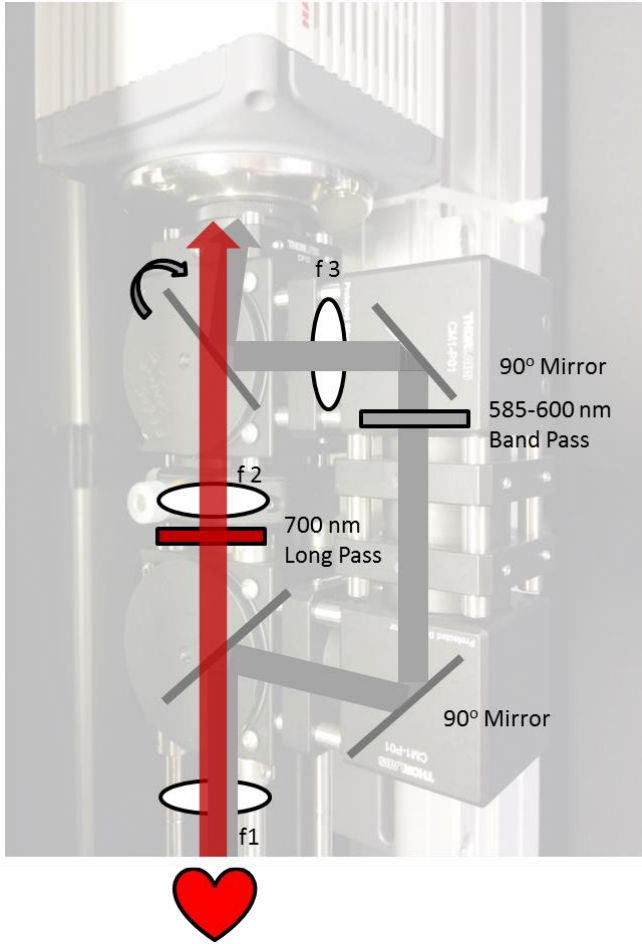


**Figure 4: Optical mapping set up showing the optical pathways**  
The red arrow follows the voltage sensitive pathway used in this study while the grey pathway indicates the spectra splitting optical pathway that transmits the calcium emission.

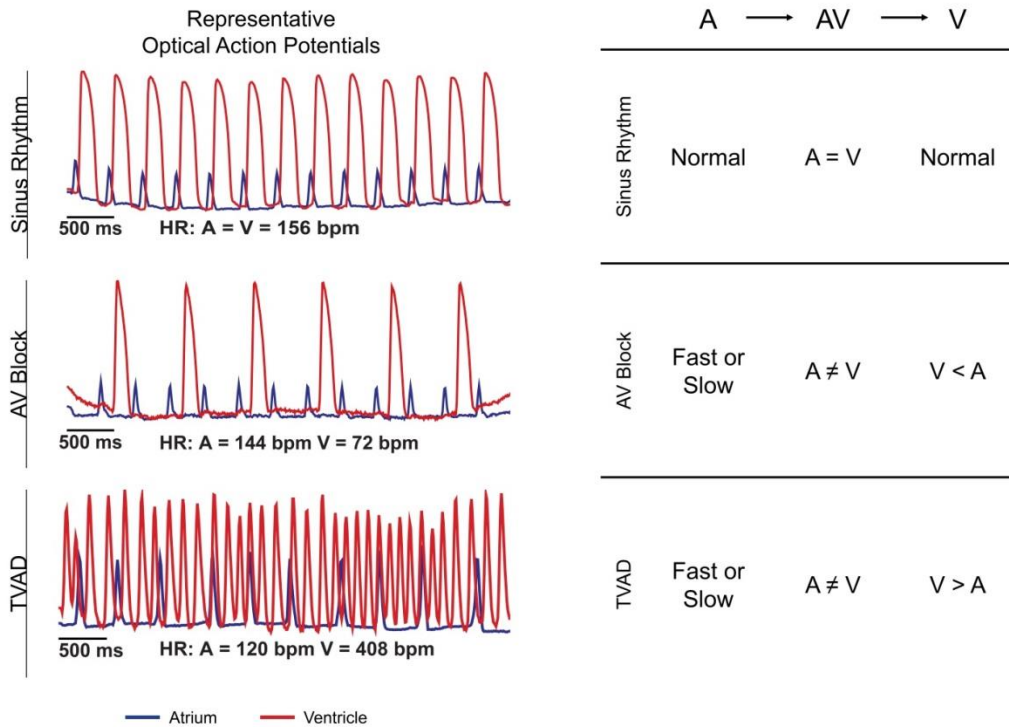


**Figure 5: Definition of arrhythmias and representative optical action potential traces.**

Left: Representative traces were obtained from regional analysis of optical data. From top to bottom, traces represent electrical events observed during the reperfusion phase. These include: Sinus rhythm, AVB, and TVAD.

Right: Definitions of arrhythmias and their conduction patterns. Table indicates the relative Atrial (A), Atrioventricular (AV), and Ventricular (V) rhythms that define the observed reperfusion arrhythmias.

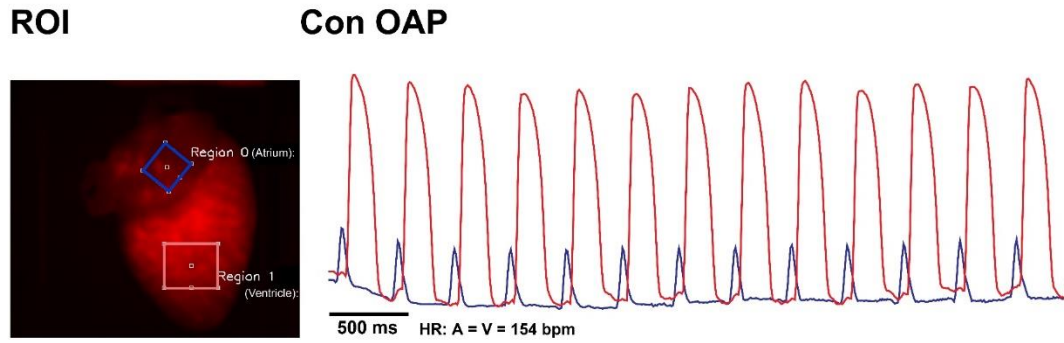


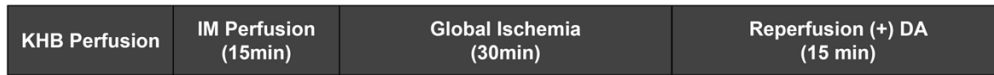
**Figure 6: Representative regions of interest (ROI) analysis and control (Con) optical action potentials (OAP).**

ROIs are drawn on the heart and the pixels within the delineated region are analyzed to produce representative results: control heart's atrial (blue) and ventricular (red) signals are shown.

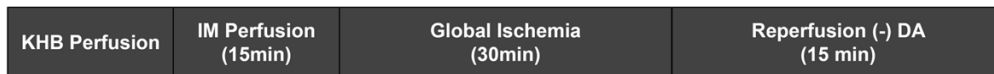
**A**



**B**



**C**



**D**

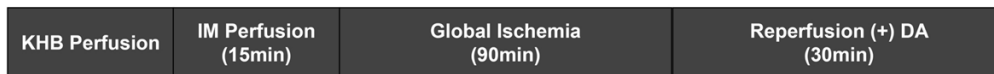


**Figure 7: Study protocols**

Time wise illustration of the four protocols: A) control experiments B) Study 1, GI 30 min, reperfusion, (-) DA C) Study 2, GI 30 min, reperfusion, (+) DA D) Study 3, GI 90 min, reperfusion (+) DA.

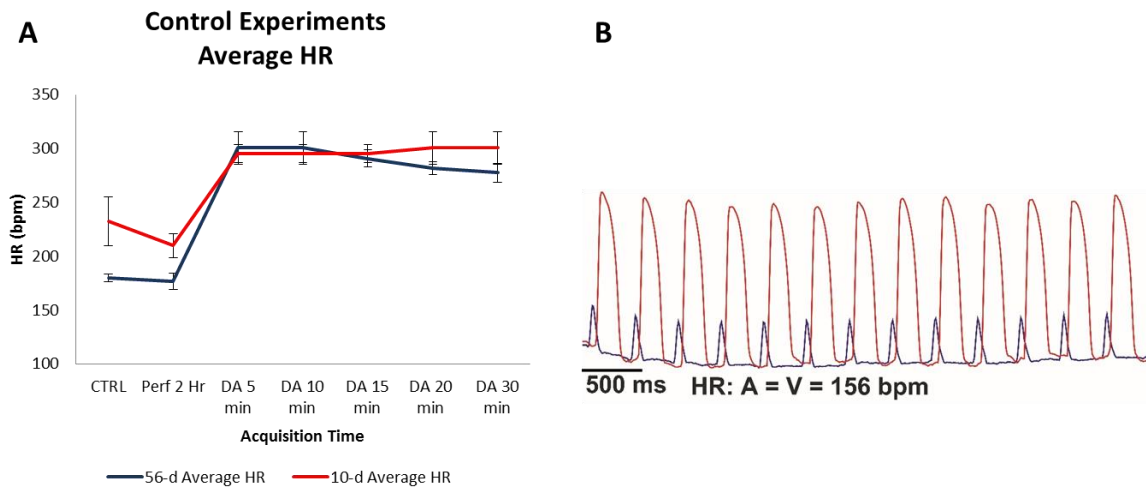


**Figure 8: Average heart rate response, in whole heart optical mapping, to control (10-d & 56-d)**  
 Average OPA frequency response to 2 hours of continuous perfusion with normal KHB solution, followed by the infusion of 20 $\mu$ M DA. Monitored for 30min post DA infusion.

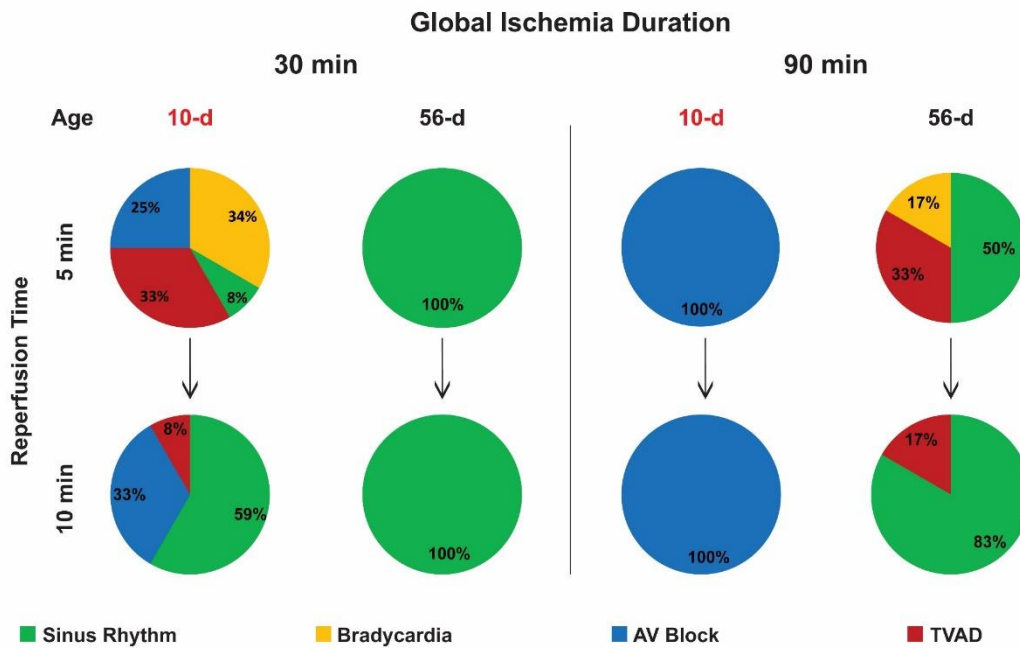


**Figure 9: Proportional representation of rhythmic responses, comparing age and ischemic duration**

Pie charts represent proportional observations of arrhythmias at 5 and 10 min of reperfusion. Comparisons are presented between two age groups (10-d vs 56-d), and between different time intervals (5 min vs 10 min) during reperfusion. The left hand section shows the results of Protocol 1 with 30 min GI and the right hand section shows the results of Protocol 2 with 90 min GI. Time is presented chronologically from the top down.



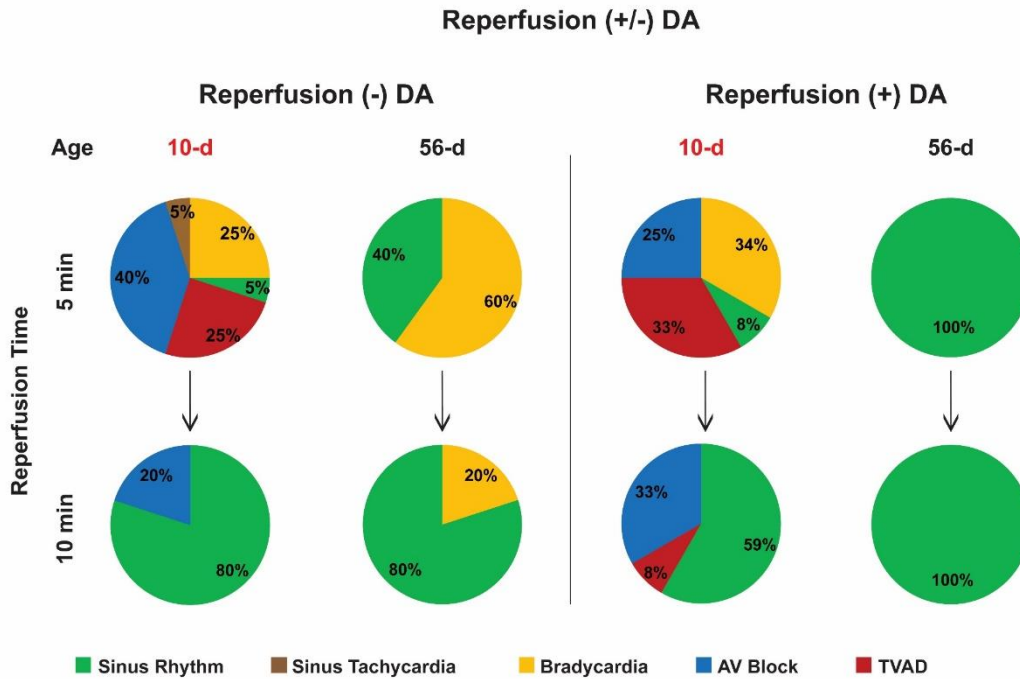


**Figure 10: Proportional representation of rhythmic responses, comparing age and post ischemia inotropy.**

Pie charts represent proportional observations of arrhythmias at 5 and 10 min of reperfusion. Comparisons are presented between two age groups (10 d vs 56 d), and between different time intervals (5 min vs 10 min) during reperfusion. Left section indicates results of (30 min GI) reperfusion without inotropic support, right section indicates results of (30 min GI) reperfusion with inotropic support. Time is presented chronologically top down.

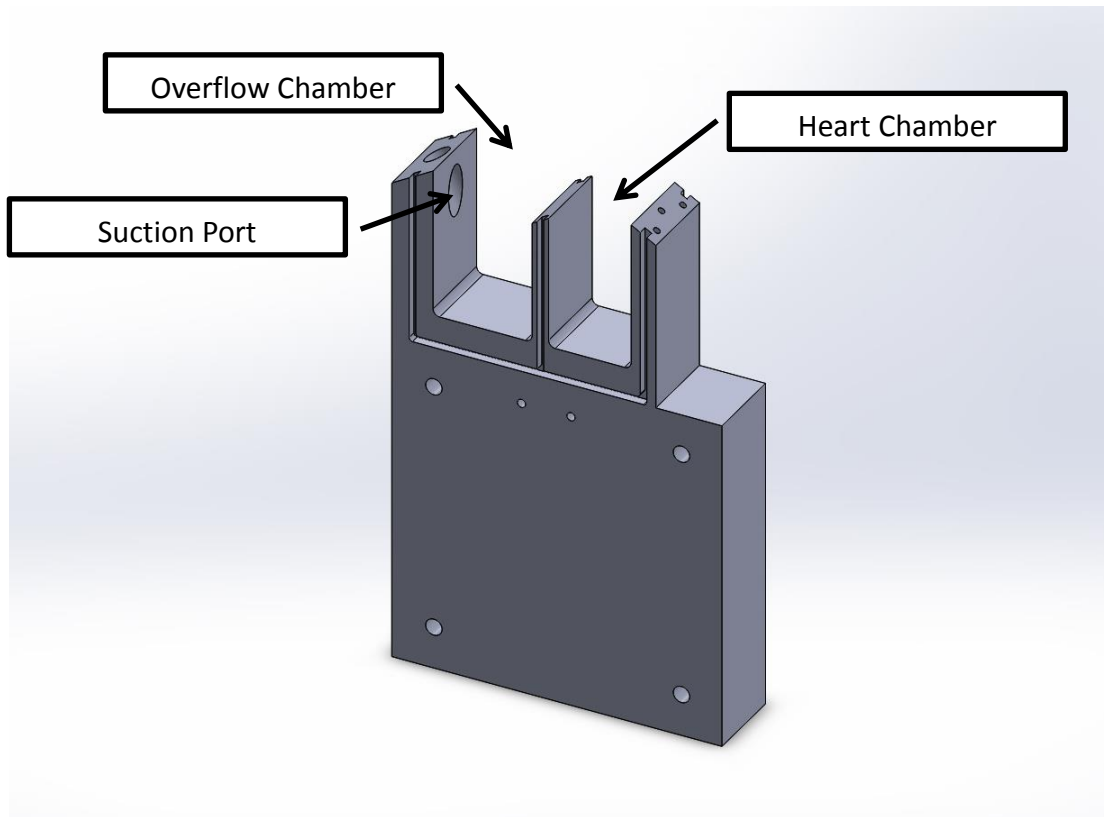


**Figure 11: Optical mapping chamber**

Custom designed optical mapping chamber using computer assisted design software Solidworks.

## References

1. Hoffman TM, Wernovsky G, Wieand TS, et al. The incidence of arrhythmias in a pediatric cardiac intensive care unit. *Pediatr Cardiol.* 2002;23(6):598-604.
2. van der Linde D, Konings EE, Slager MA, et al. Birth prevalence of congenital heart disease worldwide: a systematic review and meta-analysis. *J Am Coll Cardiol.* 2011;58(21):2241-2247.
3. Fahed AC, Gelb BD, Seidman JG, Seidman CE. Genetics of congenital heart disease: the glass half empty. *Circ Res.* 2013;112(4):707-720.
4. Burch M. Congenital heart disease. *Medicine.* 2010;38(10):561-568.
5. Khairy P, Ionescu-Iltu R, Mackie AS, Abrahamowicz M, Pilote L, Marelli AJ. Changing mortality in congenital heart disease. *J Am Coll Cardiol.* 2010;56(14):1149-1157.
6. Ou P, Iserin L, Raisky O, et al. Post-operative cardiac lesions after cardiac surgery in childhood. *Pediatr Radiol.* 2010;40(6):885-894.
7. Hayashi G, Kurosaki K, Echigo S, et al. Prevalence of arrhythmias and their risk factors mid- and long-term after the arterial switch operation. *Pediatr Cardiol.* 2006;27(6):689-694.
8. Valsangiacomo E, Schmid ER, Schüpbach RW, et al. Early postoperative arrhythmias after cardiac operation in children. *The Annals of thoracic surgery.* 2002;74(3):792-796.
9. Batra AS, Chun DS, Johnson TR, et al. A prospective analysis of the incidence and risk factors associated with junctional ectopic tachycardia following surgery for congenital heart disease. *Pediatr Cardiol.* 2006;27(1):51-55.
10. Delaney JW, Moltedo JM, Dziura JD, Kopf GS, Snyder CS. Early postoperative arrhythmias after pediatric cardiac surgery. *J Thorac Cardiovasc Surg.* 2006;131(6):1296-1300.
11. Rekawek J, Kansy A, Miszczak-Knecht M, et al. Risk factors for cardiac arrhythmias in children with congenital heart disease after surgical intervention in the early postoperative period. *J Thorac Cardiovasc Surg.* 2007;133(4):900-904.

12. Talwar S, Patel K, Juneja R, Choudhary SK, Airan B. Early postoperative arrhythmias after pediatric cardiac surgery. *Asian Cardiovasc Thorac Ann*. 2015;23(7):795-801.
13. Pfammatter J-P, Wagner B, Berdat P, et al. Procedural factors associated with early postoperative arrhythmias after repair of congenital heart defects. *The Journal of Thoracic and Cardiovascular Surgery*. 2002;123(2):258-262.
14. Zampi JD, Hirsch JC, Gurney JG, et al. Junctional ectopic tachycardia after infant heart surgery: incidence and outcomes. *Pediatr Cardiol*. 2012;33(8):1362-1369.
15. Hoffman T, Wernovsky G, Wieand T, et al. The incidence of arrhythmias in a pediatric cardiac intensive care unit. *Pediatric cardiology*. 2002;23(6):598-604.
16. Haas NA, Plumpton K, Justo R, Jalali H, Pohlner P. Postoperative junctional ectopic tachycardia (JET). *Zeitschrift fur Kardiologie*. 2004;93(5):371-380.
17. Hoffman TM, Bush DM, Wernovsky G, et al. Postoperative junctional ectopic tachycardia in children: incidence, risk factors, and treatment. *Ann Thorac Surg*. 2002;74(5):1607-1611.
18. Escudero C, Carr R, Sanatani S. The medical management of pediatric arrhythmias. *Current treatment options in cardiovascular medicine*. 2012;14(5):455-472.
19. Hoffman TM, Bush DM, Wernovsky G, et al. Postoperative junctional ectopic tachycardia in children: incidence, risk factors, and treatment. *The Annals of thoracic surgery*. 2002;74(5):1607-1611.
20. Grosse-Wortmann L, Kreitz S, Grabitz RG, et al. Prevalence of and risk factors for perioperative arrhythmias in neonates and children after cardiopulmonary bypass: continuous holter monitoring before and for three days after surgery. *J Cardiothorac Surg*. 2010;5:85.
21. Mulholland JW, Clements AT. Cardiopulmonary bypass. *Surgery (Oxford)*. 2012;30(1):19-21.
22. Chambers DJ, Fallouh HB. Cardioplegia and cardiac surgery: pharmacological arrest and cardioprotection during global ischemia and reperfusion. *Pharmacology & therapeutics*. 2010;127(1):41-52.
23. Immer FF, Stocker F, Seiler AM, et al. Troponin-I for prediction of early postoperative course after pediatric cardiac surgery. *Journal of the American College of Cardiology*. 1999;33(6):1719-1723.

24. Taggart DP, Hadjinikolas L, Hooper J, et al. Effects of age and ischemic times on biochemical evidence of myocardial injury after pediatric cardiac operations. *The Journal of Thoracic and Cardiovascular Surgery*. 1997;113(4):728-735.
25. Imura H, Caputo M, Parry A, Pawade A, Angelini GD, Suleiman M-S. Age-Dependent and Hypoxia-Related Differences in Myocardial Protection During Pediatric Open Heart Surgery. *Circulation*. 2001;103(11):1551-1556.
26. Mildh L, Hiippala A, Rautiainen P, Pettila V, Sairanen H, Happonen JM. Junctional ectopic tachycardia after surgery for congenital heart disease: incidence, risk factors and outcome. *Eur J Cardiothorac Surg*. 2011;39(1):75-80.
27. Dan P. 631 Post-ischemic effect of dopamine on pacemaker automaticity is age- and tissue-specific: A potential mechanism of Junctional Ectopic Tachycardia (JET). *Canadian Journal of Cardiology*. 2011;27(5):S291-S291.
28. Seghaye M-C. The clinical implications of the systemic inflammatory reaction related to cardiac operations in children. *Cardiology in the Young*. 2003;13(03):228-239.
29. Levi R, Owen D, Trzeciakowski J. Actions of Histamine on the. *Pharmacology of histamine receptors*. 1982:236.
30. Seghaye M-C, Duchateau J, Grabitz RG, et al. Histamine liberation related to cardiopulmonary bypass in children: Possible relation to transient postoperative arrhythmias. *The Journal of Thoracic and Cardiovascular Surgery*. 1996;111(5):971-981.
31. He G, Hu J, Li T, et al. Arrhythmogenic effect of sympathetic histamine in mouse hearts subjected to acute ischemia. *Molecular Medicine (Cambridge, Mass.)*. 2012;18:1-9.
32. Anderson RH, Yanni J, Boyett MR, Chandler NJ, Dobrzynski H. The anatomy of the cardiac conduction system. *Clinical Anatomy*. 2009;22(1):99-113.
33. Park DS, Fishman GI. The cardiac conduction system. *Circulation*. 2011;123(8):904-915.
34. Greener ID, Tellez JO, Dobrzynski H, et al. Ion channel transcript expression at the rabbit atrioventricular conduction axis. *Circ Arrhythm Electrophysiol*. 2009;2(3):305-315.
35. Ye Sheng X, Qu Y, Dan P, et al. Isolation and characterization of atrioventricular nodal cells from neonate rabbit heart. *Circ Arrhythm Electrophysiol*. 2011;4(6):936-946.

36. Efimov IR, Nikolski VP, Rothenberg F, et al. Structure-function relationship in the AV junction. *The Anatomical Record*. 2004;280A(2):952-965.
37. Bers DM. Cardiac excitation–contraction coupling. *Nature*. 2002;415(6868):198-205.
38. Mezzano V, Pellman J, Sheikh F. Cell junctions in the specialized conduction system of the heart. *Cell communication & adhesion*. 2014;21(3):149-159.
39. Kanno S, Saffitz JE. The role of myocardial gap junctions in electrical conduction and arrhythmogenesis. *Cardiovascular Pathology*. 2001;10(4):169-177.
40. Lakatta EG, Maltsev VA, Vinogradova TM. A Coupled SYSTEM of Intracellular Ca<sup>2+</sup> Clocks and Surface Membrane Voltage Clocks Controls the Timekeeping Mechanism of the Heart's Pacemaker. *Circulation Research*. 2010;106(4):659-673.
41. Biel M, Schneider A, Wahl C. Cardiac HCN Channels: Structure, Function, and Modulation. *Trends in Cardiovascular Medicine*. 2002;12(5):206-213.
42. Irisawa H, Brown HF, Giles W. Cardiac pacemaking in the sinoatrial node. *Physiological Reviews*. 1993;73(1):197-227.
43. Wilders R. Computer modelling of the sinoatrial node. *Medical & Biological Engineering & Computing*. 2006;45(2):189-207.
44. Maltsev VA, Lakatta EG. Dynamic interactions of an intracellular Ca<sup>2+</sup> clock and membrane ion channel clock underlie robust initiation and regulation of cardiac pacemaker function. *Cardiovascular Research*. 2008;77(2):274-284.
45. Noble D, Noble PJ, Fink M. Competing oscillators in cardiac pacemaking: historical background. *Circ Res*. 2010;106(12):1791-1797.
46. Atkinson AJ, Logantha SJRJ, Hao G, et al. Functional, Anatomical, and Molecular Investigation of the Cardiac Conduction System and Arrhythmogenic Atrioventricular Ring Tissue in the Rat Heart. *Journal of the American Heart Association*. 2013;2(6):e000246-e000246.
47. Hancox J, Levi A. The hyperpolarisation-activated current, I<sub>f</sub>, is not required for pacemaking in single cells from the rabbit atrioventricular node. *Pflügers Archiv*. 1994;427(1-2):121-128.
48. Ridley JM, Cheng H, Harrison OJ, et al. Spontaneous frequency of rabbit atrioventricular node myocytes depends on SR function. *Cell Calcium*. 2008;44(6):580-591.

49. Bell RM, Mocanu MM, Yellon DM. Retrograde heart perfusion: the Langendorff technique of isolated heart perfusion. *Journal of molecular and cellular cardiology*. 2011;50(6):940-950.
50. Dhein S. *The Langendorff Heart*. Springer; 2005.
51. Attin M, Clusin WT. Basic concepts of optical mapping techniques in cardiac electrophysiology. *Biological research for nursing*. 2009;11(2):195-207.
52. Dhein S, Mohr FW, Delmar M. *Practical methods in cardiovascular research*. New York;Berlin;: Springer; 2005.
53. Ayyildiz P, Kasar T, Ozturk E, et al. Evaluation of Permanent or Transient Complete Heart Block after Open Heart Surgery for Congenital Heart Disease. *Pacing and Clinical Electrophysiology*. 2016;39(2):160-165.
54. Pogwizd SM, Bers DM. Cellular basis of triggered arrhythmias in heart failure. *Trends in Cardiovascular Medicine*. 2004;14(2):61-66.
55. Carmeliet E. Cardiac ionic currents and acute ischemia: from channels to arrhythmias. *Physiological reviews*. 1999;79(3):917-1017.
56. Brown DA, O'Rourke B. Cardiac mitochondria and arrhythmias. *Cardiovascular research*. 2010;88(2):241-249.
57. Cheng H, Smith GL, Orchard CH, Hancox JC. Acidosis inhibits spontaneous activity and membrane currents in myocytes isolated from the rabbit atrioventricular node. *Journal of Molecular and Cellular Cardiology*. 2009;46(1):75-85.
58. Mohabir R, Lee H-C, Kurz RW, Clusin WT. Effects of Ischemia and Hypercarbic Acidosis on Myocyte Calcium Transients, Contraction, and pHi in Perfused Rabbit Hearts. *Circulation Research*. 1991;69(6):1525-1537.
59. Venkataraman R, Holcomb MR, Harder R, Knollmann BC, Baudenbacher F. Ratiometric imaging of calcium during ischemia-reperfusion injury in isolated mouse hearts using Fura-2. *BioMedical Engineering OnLine*. 2012;11(1):1-16.
60. Murphy E, Steenbergen C. Mechanisms Underlying Acute Protection From Cardiac Ischemia-Reperfusion Injury. *Physiol Rev*. 2008;88.
61. Imahashi K, Pott C, Goldhaber JI, Steenbergen C, Philipson KD, Murphy E. Cardiac-Specific Ablation of the Na<sup>+</sup>-Ca<sup>2+</sup> Exchanger Confers Protection Against Ischemia/Reperfusion Injury. *Circulation Research*. 2005;97(9):916-921.
62. Clusin WT. Calcium and Cardiac Arrhythmias: DADs, EADs, and Alternans. *Critical Reviews in Clinical Laboratory Sciences*. 2003;40(3):337-375.

63. Aon M, Cortassa S, Akar F, Brown D, Zhou L, O'Rourke B. From mitochondrial dynamics to arrhythmias. *The international journal of biochemistry & cell biology*. 2009;41(10):1940-1948.
64. Piper HM, Meuter K, Schäfer C. Cellular mechanisms of ischemia-reperfusion injury. *The Annals of Thoracic Surgery*. 2003;75(2):S644-S648.
65. Maier LS, Bers DM. Calcium, Calmodulin, and Calcium-Calmodulin Kinase II: Heartbeat to Heartbeat and Beyond. *Journal of molecular and cellular cardiology*. 2002;34(8):919-939.
66. Christensen MD, Dun W, Boyden PA, Anderson ME, Mohler PJ, Hund TJ. Oxidized Calmodulin Kinase II Regulates Conduction Following Myocardial Infarction: A Computational Analysis. *PLoS Computational Biology*. 2009;5(12):e1000583.
67. Hund TJ, Mohler PJ. Role of CaMKII in cardiac arrhythmias. *Trends in Cardiovascular Medicine*. 2015;25(5):392-397.
68. Laughner JI, Ng FS, Sulkin MS, Arthur RM, Efimov IR. Processing and analysis of cardiac optical mapping data obtained with potentiometric dyes. *Am J Physiol Heart Circ Physiol*. 2012;303(7):H753-765.